Option Pricing under Regime Switching (Analytical, PDE, and FFT Methods)

by

Mohammad Yousef Akhavein Sohrabi

A thesis

presented to the University of Waterloo

in fulfillment of the

thesis requirement for the degree of

Master of Mathematics

in

Computer Science

Waterloo, Ontario, Canada, 2011

I hereby declare that I am the sole author of this thesis. This is a true copy of the thesis, including any required final revisions, as accepted by my examiners.

I understand that my thesis may be made electronically available to the public.

Abstract

Although globally used in option pricing, the Black-Scholes model has not been able to reflect the evolution of stocks in the real world. A regime-switching model which allows jumps in the underlying asset prices and the parameters of the corresponding stochastic process is more accurate. We evaluate the analytical solution for pricing of European options under a two-state regime switching model. Both the convergence of the analytical solution and the feature of implied volatility are investigated through numerical examples.

We develop a number of techniques for pricing American options by solving the system of partial differential equations in a general $\mathcal{K}$-state regime-switching model. The linear complementarity problem is replaced by either the penalty or the direct control formulations. With an implicit discretization, we compare a number of iterative procedures (full policy iteration, fixed point-policy iteration, and local American iteration) for the associated nonlinear algebraic equations. Specifically, a linear system appears in the full policy iteration which can be solved directly or iteratively. Numerical tests indicate that the fixed point-policy iteration and the full-policy iteration (using a simple iteration for the linear system), both coupled with a penalty formulation, results in an efficient method. In addition, using a direct solution method to solve the linear system appearing in the full policy iteration is usually computationally very expensive depending on the jump parameters.

A Fourier transform is applied to the system of partial differential equations for pricing American options to obtain a linear system of ordinary differential equations that can be solved explicitly at each timestep. We develop the Fourier space timestepping algorithm which incorporates a timestepping scheme in the frequency domain, in which the frequency domain prices are obtained by applying the discrete Fourier transform to the spatial domain. Close to quadratic convergence in time and space is observed for

all regimes when using a second order Crank-Nicolson scheme for approximation of the explicit solution of the ordinary differential equation.

Acknowledgements

Dedication

This thesis is dedicated to the memory of my father, in honor of my mother, and to my entire family for their persistent love and support throughout my life.

Contents

List of Tables

List of Figures

List of Algorithms

Chapter 1

Introduction

1.1 Overview

There has been a tremendous demand for financial derivatives during the past few decades. These derivatives are frequently used by financial institutions to hedge risk, and hence can be viewed as a form of financial insurance. Determination of the fair market value of this insurance, and the hedging strategy used to reduce the risk in selling this insurance, is of interest in option pricing.

Most financial institutions use fairly simplistic models of asset price evolution. For instance, although the Black-Scholes model [3] has been a standard approach in option pricing, the assumptions within the model do not reflect the true behaviour of stock movements in the real world [23]. Extreme behaviour or rare events such as jumps in asset prices which may occur from time to time are not captured by the original Black-Scholes model. In addition, the assumption of constant volatility in the stochastic process is not realistic.

A stochastic process that incorporates jumps in financial parameters such as asset prices and volatilities can be employed to accomplish a more realistic model in option valuation. This achievement can be obtained by either jump-diffusion or regime-

switching models. In a jump-diffusion model, jump amplitudes of the asset are drawn from a continuum while the financial parameters remain fixed. However, the parameters that describe the stochastic process will jump between discrete values in a regime-switching model [23].

Regime-switching models are effective alternatives to traditional approaches. Compared to the common solutions, there is clear evidence suggesting that a regime-switching model is better able to capture the dynamics of long-term price evolution.

In a regime-switching market, shifts can occur in market parameters such as volatilities, stock prices, or interest rates. Those shifts can occur in more than one parameter at the same time. The unknown parameters such as volatilities that fit market data are obtained through a calibration process. This process ensures that the resulting model is consistent with the current market price information.

The rationale behind regime-switching models can be illustrated by a simplified model with only two regimes. In this model, stock prices would fluctuate between two states: high and low volatility regimes. Economic uncertainty, reorganizations, technological shifts, political issues, and other factors may cause changes in volatility of stock prices leading to a period of high volatility [27, 18]. According to Naik [27], another interpretation of regime-switching framework is that discontinuous information arrival may have a significant effect on a firm's stock prices. The volatility of stock prices would jump upwards before the arrival and revert back to its normal level after the market finds the true value of the information.

Regime-switching models can capture the aforementioned discrete shifts in market variables. Much research has been done since Hamilton [17] introduced a regime-switching model consisting of several regimes. Naik [27] proposed an analytical solution for European call options in terms of the integral of the Black-Scholes formula and the conditional density of the occupation time of the volatility process. Bollen [5] developed

2

a quadrinomial lattice to price both European and American options in a two-regime model. Hardy [18] incorporated the regime-switching model to price European options. Duan *et al.* [13] established a family of GARCH option pricing models in a regime-switching framework. Boyle and Draviam [6] compared several methods including Black-Scholes model with constant volatility, the closed-form solution proposed in Naik [27], and a PDE approach for pricing European options under a two-regime framework.

Due to the absence of a simple expression for the optimal exercise boundary, there is no closed-form solution for pricing American options. Jang [22] proposed a numerical method to approximate the value of an American put with regime-switching volatility. Le and Wang [25] proposed a computational procedure for the solution of finite time horizontal optimal stopping problems under regime-switching models including pricing of American put options. An approximate valuation was also carried out through the regime-switching framework of Barone-Adesi and Whaley [1] and by Buffington and Elliott [7]. Of those numerical approaches, Surkov [30] solved the option pricing PIDE for American options under regime-switching using Fourier time-stepping. More recently, Khaliq and Liu [24] extended the penalty method to price American options under the regime-switching framework. However, the penalty method in [24] has severe time-step restrictions.

Regime-switching models have been used in other areas. Chen and Forsyth [10] proposed a one-factor regime-switching model for the risk-adjusted natural gas spot price as an alternative to two-factor models developed by different authors (Schwartz [29] and Xu[31]). In line with this work, Chen and Insley [9] introduced a regime-switching model to improve the modeling of stochastic timber prices in optimal tree harvesting problems.

Our goal is to develop efficient methods for pricing options under a regime-switching

model, particularly for American options.

1.2   Objectives

The main objectives of this thesis are as follows:

- The analytical solution for pricing European call options under a two-state regime-switching model, derived in Naik [27], is computed using Gaussian quadrature.

- Various PDE approaches for pricing American options under a general $\mathcal{K}$-state regime-switching model are developed. We study various policy iteration methods for solution of the nonlinear discretized equations.

- The Fourier Space Time-stepping algorithm (FST), which involves Fourier-transformed PDEs with a time-stepping scheme in the frequency domain, is also employed to price American options under a general $\mathcal{K}$-state regime-switching model. Both explicit and penalty methods are developed.

- Numerical PDE results are compared with those of the analytical solution and the FST method. Specifically, we demonstrate the rates of convergence, computational costs, boundary constraints, and jump effects in each case.

Chapter 2

Analytical Solution for Option Pricing Under Regime-Switching

Closed-forms solutions for the value of European options under regime-switching have been known since the early work of Naik [27]. However, despite the profusion of research to uncover the corresponding exact solution for the value of American puts, no completely satisfactory analytic solution has been found. The problem is affected by the early-exercise feature which makes it difficult to find simple expression for the optimal exercise boundary. Nevertheless, the American put can be represented by the sum of a European put option and an early exercise premium which is expressed in terms of the unknown early exercise boundary. Using this representation, Carr [8] developed a randomization approach which yielded an analytic approximation expressing the American put value explicitly in terms of the exercise boundary. The randomization method was augmented by Jang [22] to provide an algorithm to approximate the price of an American put in the regime-switching case.

In this chapter, we validate the approach proposed in Naik [27] for pricing European options in a 2-regime case with continuous sample paths of stock prices. This solution is only applicable to the case where no jumps in the asset price occur when a regime

switch is preserved. Some type of approximation is required to extend the model to incorporate either discontinuous stock price changes or having more than 2 states in the volatility process [27].

2.1 Analytical Valuation of Contingent Claims

We assume that the volatility process has two possible states in which the volatility $\sigma(t)$ takes either a high (σ^h) or a low (σ^l) value. The asset price process has continuous sample paths which means any change in volatility is not accompanied by a jump in the asset price. The switch between two regimes can be modeled by a continuous 2-state Markov chain ($m(t) = \{h, l\}$). Let $\lambda^{h \to l} dt$ and $\lambda^{l \to h} dt$ denote the probability of shifting from regime h to l and from regime l to h over the small time period dt, respectively. Then the value of $m(t)$, which indicates the regime in which the risk adjusted asset price resides at time t, is influenced by two transition intensities ($\lambda^{h \to l}$ and $\lambda^{l \to h}$)

$$dm^{h \to l} = \begin{cases} 1 & \text{with probability } \lambda^{h \to l} dt \\ 0 & \text{with probability } 1 - \lambda^{h \to l} dt \end{cases}, \ dm^{l \to h} = \begin{cases} 1 & \text{with probability } \lambda^{l \to h} dt \\ 0 & \text{with probability } 1 - \lambda^{l \to h} dt \end{cases}$$

(2.1)

where the term $dm^{h \to l}$ and $dm^{l \to h}$ handle the transition of the Markov chain between the two states (h and l).

After incorporating a 2-state Markov-chain in the original Black-Scholes model, the regime-switching geometric Brownian motion is governed by the risk neutral process of the underlying asset price S_t:

$$\frac{dS_t}{S_t} = r dt + \sigma^{m(t)} dZ_t \tag{2.2}$$

where the superscript $m(t)$ denotes the regime at time t, and $\sigma^{m(t)}$ is the corresponding

instantaneous volatility. It can be shown that the system of option pricing PDEs for a European call option [23] can be written as

for $m_1, m_2 = h, l$:

$$\begin{cases} \frac{\partial V^{m_1}}{\partial t} + \frac{1}{2}(\sigma^{m_1})^2 S^2 \frac{\partial^2 V^{m_1}}{\partial S^2} + rS\frac{\partial V^{m_1}}{\partial S} - rV^{m_1} + \lambda^{m_1 \to m_2}(V^{m_2} - V^{m_1}) = 0, \\ V^{m_1}(S,T) = \max\{S - K, 0\}, \ m_1 \neq m_2, \ m_1 = m(t), \end{cases} \tag{2.3}$$

where $\lambda^{m_1 \to m_2}, m_1 \neq m_2$ is the transition intensity between the two regimes under the risk neutral probability measure $\mathbb{Q}$.

The analytic solution of the system of option pricing PDEs (2.3) can be expressed in closed form. For instance, to price a European call option on the stock with maturity T and exercise price K in a two-regime market, we apply the following proposition as proved in Naik [27].

Proposition 1. *Assume that the stock price process is continuous. The price of the European call option on the stock with exercise price K and maturity T, in time state (S, σ^h, t) for any contingent payoffs is given by*

$$C(S, \sigma^h, t) = \int_0^{T-t} C^* \left[S, K, r, T-t, \sqrt{\frac{s(x)}{T-t}} \right] f(x|\sigma^h) dx, \tag{2.4}$$

where $C^*(\cdot)$ is the Black-Scholes formula for call options, and

$$s(x) = (\sigma^h)^2 x + (\sigma^l)^2 (T - t - x), \ for \ 0 \leq x \leq T - t, \tag{2.5}$$

and $f(x|\sigma^h)$ denotes the conditional density of the occupation time of the volatility process in state σ^h, given that at the current moment it is in state σ^h. This density is

given by

$$f(x|\sigma^h) = e^{[-\lambda^{h\to l}x - \lambda^{l\to h}(T-t-x)]}[\delta_0(T-t-x) + g^h(x)I_1(2h(x)) + \lambda^{h\to l}I_0(2h(x))] \quad (2.6)$$

where

$$h(x) \equiv \sqrt{\lambda^{h\to l}\lambda^{l\to h}x(T-t-x)},$$

$$g^h(x) \equiv \sqrt{\lambda^{h\to l}\lambda^{l\to h}x/(T-t-x)},$$

$\delta_0(x)$ is Dirac's delta function, and $I_p(x)$ is the modified Bessel function for order p.
The call price in time state (S, σ^l, t) is the same as above except that the conditional
density $f(x|\sigma^l)$ is

$$f(x|\sigma^l) = e^{[-\lambda^{h\to l}x - \lambda^{l\to h}(T-t-x)]}[\delta_0(x) + g^l(x)I_1(2h(x)) + \lambda^{l\to h}I_0(2h(x))] \quad (2.7)$$

where

$$g^l(x) \equiv \sqrt{[\lambda^{h\to l}\lambda^{l\to h}(T-t-x)/x]},$$

and the other terms are as defined before [27].

The call option price in the above expression is an expectation of the original Black-Scholes formula in which the constant variance is replaced by the average of probabilistic variance introduced in equation (2.5). As expected, the model recovers the Black-Scholes formula in two cases; when there is no change in the variance ($\sigma^h = \sigma^l$) and when the volatility process is completely persistent ($\lambda^{h\to l} = \lambda^{l\to h} = 0$). In the second case, although the two level of volatilities are different, taking any level of volatility results in remaining in the same level in the future time intervals as the probability of shift in variances is zero.

We consider the European option on the asset price S_t with strike price K and maturity T in a two-regime market introduced in Proposition 1 . The closed-form pricing

equation (2.4) holds for any contingent payoffs in our regime-switching model. However, the analytic solution of the system of option pricing PDEs (2.3) can be computed for an arbitrary payoff $g(S_T)$ at time T. The price in time state (S, σ^h, t) of a security paying off $g(S_T)$ at the maturity date T is given by

$$C^g(S, \sigma^h, t) = e^{[-r(T-t)]} \cdot \left(\int_0^{T-t} \int_{-\infty}^{\infty} g\left[S_T(x,y)\right] n(y) f(x|\sigma^h) dy dx \right), \quad (2.8)$$

$$S_T(x,y) = \exp\left(r(T-t) - 0.5s(x) + \sqrt{\frac{s(x)}{T-t}}y \right), \quad (2.9)$$

where $s(x) = (\sigma^h)^2 x + (\sigma^l)^2 (T - t - x)$, for $0 \le x \le T - t$, and $n(y) = \frac{1}{\sqrt{2\pi}} exp(-0.5y^2)$ is the standard normal density and $f(x|\sigma^h)$ as defined above. The price of claim $g(\cdot)$ in state (S, σ^l, t) is obtained similarly using the density $f(x|\sigma^l)$.

2.2   Numerical Integration

The closed form solution of the 2-regime European option consists of a double definite integral which can be evaluated through a numerical integration process. Boyle and Draviam [6] used 101-time nodes and applied Simpson's rule to calculate the integral. The Simpson's rule provides an adequate approximation to the exact integral only if the function is relatively smooth over the specific interval. However, the above integrand represents an exponential shaped function which is better approximated by Gaussian quadrature.

2.2.1   Gaussian Quadrature

In numerical integration, Gaussian quadrature is one of the approximation algorithms to compute the numerical value of a definite integral. This rule usually obtains the best numerical estimate of an integral by picking specified points within the interval

and applying a weighted sum of function values at the points. An n-point Gaussian quadrature rule is defined as follows

$$\int_{-1}^{1} f(x)dx \approx \sum_{i=1}^{n} w_i f(x_i),$$ (2.10)

which provides an exact result for polynomials of degree equal or less than $2n - 1$ if the appropriate points (x_i) and weights (w_i) are chosen. However, this formula will only yield accurate results if the integrand $(f(x))$ is well approximated by a polynomial within the interval $[-1, 1]$. An integral over $[a, b]$ can simply be restated as an integral over $[-1, 1]$ which is given by

$$\int_{a}^{b} f(x)dx = \frac{b-a}{2} \int_{-1}^{1} f(\frac{b-a}{2}x + \frac{a+b}{2})dx \approx \frac{b-a}{2} \sum_{i=1}^{n} w_i f(\frac{b-a}{2}x_i + \frac{a+b}{2})$$ (2.11)

For the integration problem stated in (2.10), Legendre polynomials, $P_n(x)$, are associated. In this case, the i-th Gauss node, x_i, is the i-th root of P_n and its weight is as the following

$$\begin{cases} w_i = \frac{2}{(1-x_i)^2[P_n'(x_i)]^2}, \\ P_n(x) = \frac{1}{2^n n!}\frac{d^n}{dx^n}\left[(x^2-1)^n\right]. \end{cases}$$ (2.12)

Other choices of $[a, b]$ and the integrand lead to some extensions of the basic rule of Gaussian quadrature. Consequently, introducing a positive weight function into the integrand gives us the general form

$$\int_{a}^{b} \omega f(x)dx \approx \sum_{i=1}^{n} w_i f(x_i).$$

For some specific values of $[a, b]$ and ω, extended integration rules can be applied. For

10

instance, Gauss–Laguerre quadrature is a special case with the following form

$$\int_0^{+\infty} e^{-x} f(x) dx \approx \sum_{i=1}^n w_i f(x_i), \qquad (2.13)$$

where x_i is the i-th root of Laguerre polynomial $L_n(x)$ and the weight w_i is given by

$$\begin{cases} w_i = \frac{x_i}{(n+1)^2 [L_{n+1}(x_i)]^2}, \\[2mm] L(x) = \frac{e^x}{n!} \frac{d^n}{dx^n} (e^{-x} x^n). \end{cases} \qquad (2.14)$$

2.2.2   Evaluation Process

We evaluated (2.8) numerically using the appropriate forms of Gaussian quadrature. To make it easier to follow the calculation process, we define

$$\hat{g}(x, y) = g(S_T(x, y)) n(y),$$

where $S_T(x, y)$ is given in equation (2.9), $g(S_T(x, y))$ is the option payoff introduced in (2.8), and $n(y)$ is the standard normal density. Now, the double integral in the call option pricing formula (2.8) can be expressed in a general form given by

$$\begin{aligned} D_I &= \int_0^{T-t} f(x|\sigma^h) \left[\int_{-\infty}^{\infty} \hat{g}(x, y) dy \right] dx \\ &= \int_0^{T-t} f(x|\sigma^h) \underbrace{\left[\int_{-\infty}^0 \hat{g}(x, y) dy + \int_0^{\infty} \hat{g}(x, y) dy \right]}_{G(x)} dx \\ &= \int_0^{T-t} \underbrace{f(x|\sigma^h) G(x)}_{h(x)} dx, \end{aligned}$$

11

where, $G(x)$ is the output of the inner integral for a specific value of x in the interval $[0, T - t]$. Applying the main Gaussian quadrature rule to D_I, as in (2.10) and (2.11), gives

$$D_I = \int_0^{T-t} h(x) dx$$
$$= \frac{T-t}{2} \sum_{i=1}^{n_1} w_{x_i} h(\frac{T-t}{2} x_i + \frac{T-t}{2}),$$
$$= \frac{T-t}{2} \sum_{i=1}^{n_1} w_{x_i} h(X_i), \ X_i = \frac{T-t}{2} x_i + \frac{T-t}{2},$$

where the Gauss node x_i and its weight w_{x_i} has been given in (2.12), and n_1 is the number of points used to approximate the outer integral, $h(x)$. To evaluate $h(x)$, we have to compute the inner integral, $G(x)$, where the integrand is a function of both x and y, and x is from the outer integral, i.e. x_i. Therefore

$$G(X_i) = \int_{-\infty}^0 \hat{g}(X_i, y) dy + \int_0^\infty \hat{g}(X_i, y) dy,$$
$$X_i = \frac{T-t}{2} x_i + \frac{T-t}{2},$$

$$x_i \text{ is the Gauss node of the outer integral.}$$

Multiplying $G(X_i)$ by $e^{-y} e^y = 1$ gives

$$G(X_i) = \int_{-\infty}^0 e^{-y} \left(e^y \hat{g}(X_i, y) \right) dy + \int_0^\infty e^{-y} \left(e^y \hat{g}(X_i, y) \right) dy,$$

and by a variable change from y to $-y$ in the first interval $[0, -\infty]$, we have

$$G(X_i) = \overbrace{- \int_0^\infty e^{-y} \underbrace{\left(e^y \hat{g}(X_i, -y) \right)}_{g_1^i(y)} dy}^{G_1(X_i)} + \overbrace{\int_0^\infty e^{-y} \underbrace{\left(e^y \hat{g}(X_i, y) \right)}_{g_2^i(y)} dy}^{G_2(X_i)}. \qquad (2.15)$$

12

These changes enables us to use the Gauss–Laguerre quadrature rule, as in (2.13), in the following way

$$G(X_i) = -\sum_{j=1}^{n_2} w_{y_j} g_1^i(y_j) + \sum_{j=1}^{n_2} w_{y_j} g_2^i(y_j),$$

$$g_1^i(y) = e^y \hat{g}(X_i, -y), \ g_2^i(y) = e^y \hat{g}(X_i, y),$$

where the Gauss node y_j and its weight w_{y_i} has been given in (2.14), and n_1 is the number of points used to approximate the two integrals, $G_1(X_i)$ and $G_2(X_i)$. Therefore, the whole algorithm can be expressed in the following two steps:

1. Applying the general form of Gaussian quadrature to the outer integral to extract the values of x_i and their corresponding weights w_{x_i}, where $i = 1, ..., n_1$.

2. Applying Gaussian-Laguerre quadrature to the inner integral for each value of x_i ($i = 1, ..., n_1$) to extract the values of y_j and their corresponding weights w_{y_j}, where $j = 1, ..., n_2$.

$$
\begin{aligned}
D_I &= \int_0^{T-t} h(x)dx \\
&= \frac{T-t}{2} \sum_{i=1}^{n_1} \{w_{x_i} h(X_i)\} \\
&= \frac{T-t}{2} \sum_{i=1}^{n_1} \left\{ w_{x_i} \left[f(X_i|\sigma^h) G(X_i) \right] \right\} \\
&= \frac{T-t}{2} \sum_{i=1}^{n_1} \left\{ w_{x_i} f(X_i|\sigma^h) \left[-\sum_{j=1}^{n_2} w_{y_j} g_1^i(y_j) + \sum_{j=1}^{n_2} w_{y_j} g_2^i(y_j) \right] \right\} \quad (2.16)
\end{aligned}
$$

The accuracy of the results when using Gaussian quadrature formula is usually improved by increasing the number of points. Nevertheless, the rate of convergence of the evaluation process depends substantially on the nature of the integrand [2]. For instance, the non-smooth shape of the payoff function for European options influences

13

the rate of convergence. However, we can remove the non-smooth part of the payoff from the integrands in (2.15). It can be shown that

$$
\begin{cases}
g_1^i(y) \equiv 0 & \exists \tilde{y}_1^i, \ \forall y \leq \tilde{y}_1^i \\
g_2^i(y) \equiv 0 & \exists \tilde{y}_2^i, \ \forall y \leq \tilde{y}_2^i
\end{cases} .
$$

Since

$$
\begin{aligned}
g_1^i(y) &= e^y \hat{g}(X_i, -y) \\
&= e^y g(S_T(X_i, -y)) n(-y) \\
&= e^y \left\{ \max(S_T(X_i, -y) - K, 0) \right\} n(y),
\end{aligned}
$$

where $n(-y) = n(y)$, $\forall y$, as the standard normal density function $n(y)$ is symmetric around point $y = 0$. The payoff $g(S_T(X_i, y))$, in which S_T depends on both X_i and y (2.9), is zero for all $S_T \leq K$. Recall that S_T, at the fixed point X_i, depends only on y so that the payoff function gives a point of non-smoothness at $\tilde{y}_1^i = 0$. A similar behaviour for $g_2^i(y)$ is observed in the second integrand (2.15). As a result, we have

$$
\begin{aligned}
G(X_i) &= \left[-\int_0^{\tilde{y}_1^i} \overbrace{e^{-y} g_1^i(y) dy}^{0} + \int_{\tilde{y}_1^i}^{\infty} e^{-y} g_1^i(y) dy \right] + \left[\int_0^{\tilde{y}_2^i} \overbrace{e^{-y} g_2^i(y) dy}^{0} + \int_{\tilde{y}_2^i}^{\infty} e^{-y} g_2^i(y) dy \right] . \\
&= \int_{\tilde{y}_1^i}^{\infty} e^{-y} g_1^i(y) dy + \int_{\tilde{y}_2^i}^{\infty} e^{-y} g_2^i(y) dy
\end{aligned}
$$

With these variations, applying a general form of Gauss–Laguerre quadrature rule where the lower bound of the interval is a non-zero value (i.e. $\tilde{y}_1$ or $\tilde{y}_2$) gives us

$$G(X_i) = -\sum_{j=1}^{n_2} w_{y_j} g_1^i(y_j + \tilde{y}_1^i) + \sum_{j=1}^{n_2} w_{y_j} g_2^i(y_j + \tilde{y}_2^i)$$

Consequently, by using this expression for $G(x_i)$, equation (2.16) can be rewritten as

$$D_I = \frac{T-t}{2} \sum_{i=1}^{n_1} \left\{ w_{x_i} f(X_i | \sigma^h) \left[-\sum_{j=1}^{n_2} w_{y_j} g_1^i(y_j + \tilde{y}_1^i) + \sum_{j=1}^{n_2} w_{y_j} g_2^i(y_j + \tilde{y}_2^i) \right] \right\} \quad (2.17)$$

which, as we will see, results in smooth convergence.

2.2.3   Observations

Having introduced the two-step Gaussian quadrature approach for computing the double integral in the previous section, this section conducts numerical observations based on the proposed algorithm. To accomplish an accurate study, we present analytical solution results for European call option prices with different sets of parameters. As stated earlier, the accuracy of the process depends on the number of points used to solve the integral numerically. Having computed a double integral, we used different pairs of numbers to obtain the best combination leading to precise outcomes. Analytical results are given when there are two hidden Markov states (a high-volatility regime and a low-volatility regime) with the values of regime parameters summarized in Table 2.1. In addition, the structure of implied volatility (i.e. the smile/skew) provides us a tool to validate the analytical approach. Therefore, we examine the capability of our model to produce the volatility smile/skew in the market.

Parameter	Value	Parameter	Value
r	0.05	S	100\$
T	$1\ year$	K	100\$
σ^h	$0.25(1/\sqrt{year})$	$\lambda^{h\to l}$	0.5
σ^l	$0.15(1/\sqrt{year})$	$\lambda^{l\to h}$	0.5

Table 2.1: *Input parameters used to price European options under the two-state regime-switching model of the analytical solution, where and are transition intensities for state h to l (high to low), and state l to h (low to high), respectively.*

2.2.3.1 Accuracy Analysis

We first carry out an accuracy analysis, assuming that the European call option pricing model in (2.8) is evaluated by (2.17) using input financial parameters in Table 2.1. The preciseness of the results is influenced by non-financial parameters such as the number of points chosen for the numerical computation of the inner integral, n_1, and the outer integral, n_2. More accuracy can be sought by increasing the number of points. This fact can be seen in the top part of Table 2.2 where n_1 and n_2 are initiated by 2 in the first step and are doubled in the next stage. However, we found that there is an optimal measure for n_1 which provides the same results compared with those obtained by increasing n_1 in each step. The bottom part of Table 2.2 gives the values when n_1 is constant and fixed at 8. It can be observed that the two strategies are equivalent up to 10-digit precision after the second step, i.e. the third row in the both parts of Table 2.2, where n_1 remains at 8 (bottom) and continues to be doubled (top). In fact, finding the optimal number of points in the outer integral implies that the integrand can be well approximated by a polynomial of degree $2n_1 - 1 = 15$ within the interval $[0, T - t]$.

$$(n_1 = 2^n,\ n = \{1, .., 7\})$$

		Regime h ($h$igh volatility)			Regime l ($l$ow volatility)		
n_1	n_2	Option Value	Change	Ratio	Option Value	Change	Ratio
2	**2**	**8.4023763060**			**6.4590712570**		
4	**4**	**12.4709531800**	**4.06857687**		**10.0409693100**	**3.58189805**	
8	8	11.6598247800	**0.81112840**	5.02	9.3144369340	**0.72653238**	4.93
16	16	11.7063144100	0.04648963	17.45	9.3404781310	0.02604120	27.90
32	32	11.7050731600	0.00124125	37.45	9.3392516890	0.00122644	21.23
64	64	11.7050718400	0.00000132	940.34	9.3392501610	0.00000153	802.65
128	128	11.7050718400	0.00000000	N A	9.3392501610	0.00000000	N A

$$(n_1 = 2^3)$$

		Regime h ($h$igh volatility)			Regime l ($l$ow volatility)		
n_1	n_2	Option Value	Change	Ratio	Option Value	Change	Ratio
8	**2**	**8.4024813390**			**6.4591999650**		
8	**4**	**12.4709530600**	**4.06847172**		**10.0409687800**	**3.58176882**	
8	8	11.6598247800	**0.81112828**	5.02	9.3144369340	**0.72653185**	4.93
8	16	11.7063144100	0.04648963	17.45	9.3404781310	0.02604120	27.90
8	32	11.7050731600	0.00124125	37.45	9.3392516890	0.00122644	21.23
8	64	11.7050718400	0.00000132	940.34	9.3392501610	0.00000153	802.65
8	128	11.7050718400	0.00000000	N A	9.3392501610	0.00000000	N A

Table 2.2: *The accuracy analysis of the two-step Gaussian quadrature approach used for the two-state regime-switching model of the European call pricing in [27], where n_1 and n_2 are the number of points chosen for the numerical computation of the first and second integral, respectively. The results are shown in two parts: top, where both n_1 and n_2 are increasing, and bottom, where n_1 is fixed at 8 and n_2 is increasing.*

2.2.3.2   Implied Volatility

According to the original Black-Scholes model, the volatility for both call and put options is constant across all possible strike prices K and maturity times T. However, the constant volatility assumption is not consistent with the real behaviour of the options market where the volatility implied by the market price depends on both K and T. Regime-switching models capture better this feature of implied volatility. This smile/skew, results from plotting the strike price and implied volatility of options with the same expiration date.
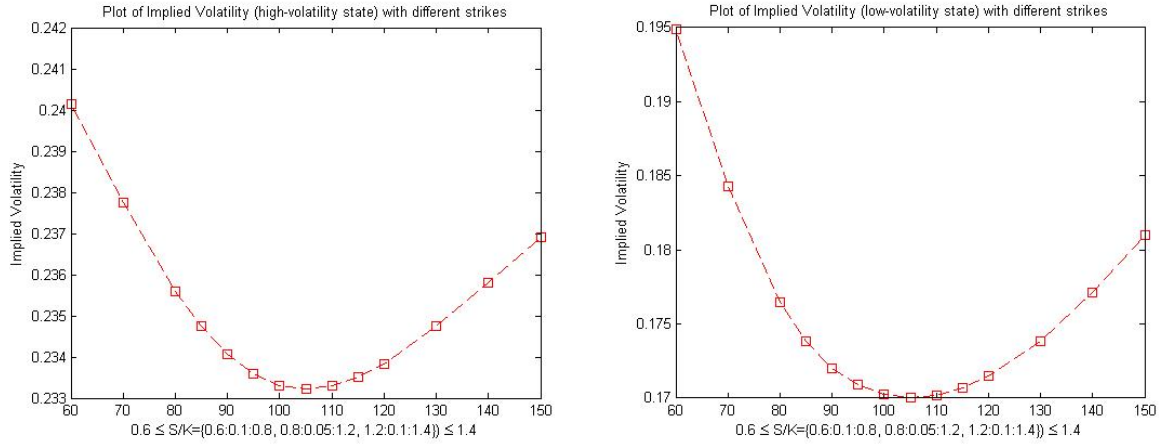
Figure 2.1: *Implied volatilities generated by using one-year European call option values from a two-state regime-switching model as the market prices. In the left panel, the call options are priced assuming the current regime is the high-volatility state; In the right panel, the current regime is assumed the low-volatility state. The high- and low-state parameters are volatilities $\sigma^h = 0.25$ and $\sigma^l = 0.15$ with intensities $\lambda^{h \to l} = 0.5$ and $\lambda^{l \to h} = 0.5$, and interest rate r=0.05.*

We treat the option values from a two-state regime-switching model as the market prices. The next step is to find those volatilities in the Black-Scholes model yielding option values equal to the market prices. Given five out of six parameters in the Black-Scholes model, i.e. market option value V, stock price S, strike price K, interest rate r, and expiry time T, implied volatilities are derived and plotted in Figure 2.1. In our simplified model, where jumps are not allowed, skews cannot be generated.

Chapter 3

PDE Methods for Option Pricing under Regime-switching Processes

3.1   Introduction

In this chapter, we develop different approaches for numerically solving the system of option pricing PDEs for pricing American options under regime switching. We begin with existing techniques for pricing European options under regime-switching processes as in [23]. Having employed both iterative and direct solution methods for solving the discretized PDEs in pricing European-style options, we will investigate various algorithms for American options.

We assume a market with discrete random shifts in the volatility process and $\left\{\sigma^1, \ldots, \sigma^{\mathcal{K}}\right\}$ as the possible values of the volatility. A simple way to capture switching between regimes is using continuous Markov chains. Let M_t be a continuous $\mathcal{K}$-state Markov chain taking values in the state space $\{1, 2, 3, ..., \mathcal{K}\}$, where $\mathcal{K}$ is the total number of regimes. The continuous Markov chain M_t is specified by its rate matrix Q. According to the theory, the entries q_{kl} in Q must satisfy the following equations:

1. off-diagonal entries: $q_{kl} \geq 0$ if $k \neq l$

2. diagonal entries: $q_{kk} \leq 0$ and $q_{kk} = -\sum_{l=1,l\neq k}^{\mathcal{K}} q_{kl}$

Off-diagonal entries are known as transitional intensities. After incorporating a $\mathcal{K}$-state Markov-chain in the original Black-Scholes model, the regime-switching model is governed by the following process under the real world probability measure ($\mathbb{P}$-measure):

$$dS = (\alpha^k - \tilde{\eta}^k)Sdt + \sigma^k SdZ + \sum_{l=1}^{\mathcal{K}} S(\eta^{kl} - 1)dM^{kl} \tag{3.1}$$

where the superscripts denote regime numbers, and α^k and σ^k are the corresponding instantaneous expected return and volatility. In addition, η^{kl} is the size of jump in the underlying S when the regime changes from state k to state l, i.e. S would jump from S to $S\eta^{kl}$. The term dM^{kl} handles the transition of the Markov chain between different states (k and l) so that

$$dM^{kl} = \begin{cases} 1 & \text{with probability } \lambda^{kl}dt + \delta^{kl} \\ 0 & \text{with probability } 1 - \lambda^{kl}dt - \delta^{kl} \end{cases}, \tag{3.2}$$

where $\lambda^{kl} \geq 0$ is the transition intensity (the same definition as q_{kl}) for state k to l when $k \neq l$, δ^{kl} is the time-independent term of the probability of shifting from regime k to l, and

$$\lambda^{kk} = -\sum_{l=1,l\neq k}^{\mathcal{K}} \lambda^{kl}. \tag{3.3}$$

Besides that, $\tilde{\eta}^k$ is the instantaneous expected return due to all jumps out of state k so that

$$\tilde{\eta}^k = \sum_{l=1,l\neq k}^{\mathcal{K}} \lambda^{kl}(\eta^{kl} - 1) = \sum_{l=1}^{\mathcal{K}} \lambda^{kl}\eta^{kl} \tag{3.4}$$

It is assumed that $\eta^{kk} = 1$ which means a jump in the asset price will occur only if

20

there is a transition between state k and state l. However, it is possible to allow a jump without a change in regime. In that case, jump may happen any time and can be modeled by introducing a compound Poisson process in (3.1) [23]. It can be shown [23] that the system of option pricing PDEs for a European put option under the risk neutral probability measure ($\mathbb{Q}$) can be written as

for $k = 1, 2, 3, ..., \mathcal{K}$:

$$
\begin{cases}
\frac{\partial V^k}{\partial t} + \frac{1}{2}(\sigma^k)^2 S^2 \frac{\partial^2 V^k}{\partial S^2} + (r - \eta_k^{\mathbb{Q}})S\frac{\partial V^k}{\partial S} - rV^k + \sum_{l=1,l\neq k}^{\mathcal{K}} \lambda_{kl}^{\mathbb{Q}}(V^l(S\eta^{kl}) - V^k) = 0, \\
V^k(S,T) = \max\{K - S, 0\}
\end{cases}
\tag{3.5}
$$

where $\lambda_{kl}^{\mathbb{Q}} \geq 0$ and $\eta_k^{\mathbb{Q}}$ are the risk-adjusted values of the transition intensity (λ^{kl}) and the instantaneous expected return ($\tilde{\eta}^k$), respectively. Under the $\mathbb{Q}$-measure, equations (3.3 and 3.4) are replaced by

$$
\lambda_{kk}^{\mathbb{Q}} = -\sum_{l=1,l\neq k}^{N} \lambda_{kl}^{\mathbb{Q}}; \quad \hat{\eta}_k{}^{\mathbb{Q}} = \sum_{l=1}^{N} \lambda_{kl}^{\mathbb{Q}} \eta^{kl}.
\tag{3.6}
$$

Kennedy [23] developed a simple iterative method to find the European option prices for (3.5).

Khaliq and Liu [24] solved the above coupled system of PDEs for an American put option by extending the penalty method to the $\mathcal{K}$-regime case and developing numerical schemes via an implicit θ-method. The penalty function that they added to (3.5) was:

$$
\frac{\epsilon C}{V_\epsilon^k(S,t) + \epsilon - q(S)}, i = 1, ..., \mathcal{K}, \text{ and } q(S) = K - S,
\tag{3.7}
$$

where $0 < \epsilon << 1$ is a small regularization parameter and $C > 0$ is a fixed constant. However, the method has severe time-step restrictions. The idea of penalty method was originally proposed by Zvan *et al.* [34] for the original Black-Scholes model.

3.2   Numerical Solution for the Option-Pricing PDEs

3.3   System of Option-Pricing PDEs

Given that $\tau = T - t$, the system of option-pricing PDEs introduced in Section 3.1 can be rewritten as

$$\frac{\partial V^k}{\partial \tau} = \frac{1}{2}(\sigma^k)^2 S^2 \frac{\partial^2 V^k}{\partial S^2} + (r - \tilde{\eta}_k{}^{\mathbb{Q}})S \frac{\partial V^k}{\partial S} - \left(r - \lambda_{kk}^{\mathbb{Q}}\right) V^k + \sum_{l=1,l\neq k}^{\mathcal{K}} \lambda_{kl}^{\mathbb{Q}} V^l(S\eta^{kl}). \quad (3.8)$$

The initial condition for the system of equations (3.8) is given by the option payoff when $\tau = 0$

$$V^k(S,0) = V_*(S), \ k = 1,\ldots,\mathcal{K}. \quad (3.9)$$

The system of equations (3.8) is placed on the localized domain

$$(S,\tau) \in [0, S_{max}] \times [0,T]. \quad (3.10)$$

No boundary condition is required at $S = 0$ where the system of PDEs simply reduces to

$$\frac{\partial V^k}{\partial \tau} = - \left(r - \lambda_{kk}^{\mathbb{Q}}\right) V^k + \sum_{l=1,l\neq k}^{\mathcal{K}} \lambda_{kl}^{\mathbb{Q}} V^l(S\eta^{kl}). \quad (3.11)$$

At $S = S_{max}$, the payoff (3.9) is imposed as a Dirichlet condition. However, the system may require option values for $S > S_{max}$ when the relative jump size is greater than one. To solve this numerical problem, we replace the jump term η^{kl} with an augmented jump amplitude near S_{max} as in [23],

$$\bar{\eta}^{kl}(S) = \begin{cases} \eta^{kl} & 0 \leq S \leq \frac{S_{max}}{\eta^{kl}} \\[2mm] \frac{S_{max}}{S} & \frac{S_{max}}{\eta^{kl}} \leq S \leq S_{max}, \end{cases} \quad (3.12)$$

where $S\bar{\eta}^{kl}$ is always within $[0, S_{max}]$. Furthermore, the risk-adjusted instantaneous expected return $(\hat{\eta}_k{}^{\mathbb{Q}})$ introduced in (3.6) is no longer constant and can be rewritten as

$$\hat{\eta}_k{}^{\mathbb{Q}} = \sum_{l=1}^{\mathcal{K}} \lambda_{kl}^{\mathbb{Q}} \bar{\eta}^{kl}(S). \tag{3.13}$$

3.4   Discretization of the PDEs

We follow the same procedure for discretization as discussed in [23]. The localized system of PDEs in (3.8) to $[0, S_{max}] \times [0, T]$ can be discretized using an implicit method. With the following notations

$$
\begin{array}{lll}
k & \text{regime number} & (1, \ldots, \mathcal{K}) \\
m & \text{timestep index} & (1, \ldots, \mathcal{M}) \\
n & \text{asset node index} & (1, \ldots, \mathcal{N}),
\end{array}
$$

the option value at timestep m for regime k and asset price S_n is represented by $V_{m,n}^k$. We define the vector of option values at timestep m for regime k as

$$V_m^k = \left[V_{m,1}^k, V_{m,2}^k, \ldots, V_{m,\mathcal{N}}^k \right]^{\mathrm{T}}. \tag{3.14}$$

and the matrix of option values at timestep m

$$V_m = \left[V_m^1, V_m^2, \ldots, V_m^{\mathcal{K}} \right]. \tag{3.15}$$

The discrete equations for regime k are given by

$$\left[I + \theta\Delta\tau(\alpha_n^k + \beta_n^k + r - \lambda_{kk}^{\mathbb{Q}})\right] V_{m+1,n}^k - \theta\Delta\tau\alpha_n^k V_{m+1,n-1}^k - \theta\Delta\tau\beta_n^k V_{m+1,n+1}^k$$

$$= \left[I - (1-\theta)\Delta\tau(\alpha_n^k + \beta_n^k + r - \lambda_{kk}^{\mathbb{Q}})\right] V_{m,n}^k$$

$$+ (1-\theta)\Delta\tau\alpha_n^k V_{m,n-1}^k + (1-\theta)\Delta\tau\beta_n^k V_{m,n+1}^k$$

$$+ (1-\theta)\Delta\tau \sum_{l=1,l\neq k}^{\mathcal{K}} \lambda_{kl}^{\mathbb{Q}}\mathcal{I}_{n,k,l}\left(V^l(S_n\bar{\eta}^{kl}, \tau_m)\right)$$

$$+ \theta\Delta\tau \sum_{l=1,l\neq k}^{\mathcal{K}} \lambda_{kl}^{\mathbb{Q}}\mathcal{I}_{n,k,l}\left(V^l(S_n\bar{\eta}^{kl}, \tau_{m+1})\right). \qquad (3.16)$$

Since $S_n\bar{\eta}^{kl}$ is not necessarily coincident with the asset nodes, we approximate $V^l(S_n\bar{\eta}^{kl}, \tau_m)$ by linear interpolation. We choose n^* so that

$$S_{n_l^*} < S_n\bar{\eta}^{kl} < S_{n_l^*+1}. \qquad (3.17)$$

The interpolation is represented by

$$\mathcal{I}_{n,k,l}\left(V_m^l\right) = wV_{m,n_l^*}^l + (1-w)V_{m,n_l^*+1}^l, \ w \in [0,1]. \qquad (3.18)$$

We use central differencing as much as possible at each time step, since it is more accurate. However, if α_n^k and β_n^k are negative, oscillations may occur in the solution and either forward or backward differencing can be used as the alternatives. Therefore,

24

α_n^k and β_n^k for $n = 2, \ldots, \mathcal{N} - 1$ can be chosen from

$$
\begin{aligned}
\alpha_{n,central}^k &= \frac{(\sigma^k)^2 S_n^2}{(S_n - S_{n-1})(S_{n+1} - S_{n-1})} &- \frac{(r - \hat{\eta_k}^{\mathbb{Q}}(S_n))S_n}{S_{n+1} - S_{n-1}} \\
\beta_{n,central}^k &= \frac{(\sigma^k)^2 S_n^2}{(S_{n+1} - S_n)(S_{n+1} - S_{n-1})} &+ \frac{(r - \hat{\eta_k}^{\mathbb{Q}}(S_n))S_n}{S_{n+1} - S_{n-1}} \\
\alpha_{n,forward}^k &= \frac{(\sigma^k)^2 S_n^2}{(S_n - S_{n-1})(S_{n+1} - S_{n-1})} & \\
\beta_{n,forward}^k &= \frac{(\sigma^k)^2 S_n^2}{(S_{n+1} - S_n)(S_{n+1} - S_{n-1})} &+ \frac{(r - \hat{\eta_k}^{\mathbb{Q}}(S_n))S_n}{S_{n+1} - S_n} \\
\alpha_{n,backward}^k &= \frac{(\sigma^k)^2 S_n^2}{(S_n - S_{n-1})(S_{n+1} - S_{n-1})} &- \frac{(r - \hat{\eta_k}^{\mathbb{Q}}(S_n))S_n}{S_n - S_{n-1}} \\
\beta_{n,backward}^k &= \frac{(\sigma^k)^2 S_n^2}{(S_{n+1} - S_n)(S_{n+1} - S_{n-1})} &
\end{aligned}
\tag{3.19}
$$

The discrete equations (3.16) has been given for the asset nodes within $[S_2, \ldots, S_{\mathcal{N}-1}]$. However, the reduced system (3.11) for the boundary condition $S = S_1 = 0$ can still be handled by (3.16), if we choose $\alpha_1^k = \beta_1^k = 0$. The upper limit of the boundary condition, $S = S_{\mathcal{N}} = S_{max}$, is imposed through the payoff as a Dirichlet condition

$$
V_{m+1,\mathcal{N}}^k = V_*^k, \ k = 1, \ldots, \mathcal{K}
\tag{3.20}
$$

3.5   Solving Discrete Equations

Given the vector of option values in regime k at time τ_m (3.14), the discrete equations (3.16) for regime k can be written in matrix form as

$$
\left[I - \theta M^k \right] V_{m+1}^k = \left[I + (1 - \theta)M^k \right] V_m^k + (1-\theta)\Delta\tau \Xi(V_m^k) + \theta\Delta\tau \Xi(V_{m+1}^k), \ k = 1, \ldots, \mathcal{K},
\tag{3.21}
$$

where

$$
\left[M^k V_m^k \right]_{row \ n} = \Delta\tau \left[\alpha_n^k V_{m,n-1}^k - (\alpha_n^k + \beta_n^k + r - \lambda_{kk}^{\mathbb{Q}})V_{m,n}^k + \beta_m^k V_{m,n+1}^k \right]
$$

and

$$\Xi(V_m^k) = \tilde{V}_m \lambda_k^{\mathbb{Q}} = \left[\left[\tilde{V}_m^1 \right] \cdots \underbrace{\left[\tilde{V}_m^k \right]}_{k^{th} \ vector} \cdots \left[\tilde{V}_m^{\mathcal{K}} \right] \right]_{\mathcal{N} \times \mathcal{K}} \left[\lambda_{k1}^{\mathbb{Q}}, \ldots, \underbrace{0}_{k^{th} \ element}, \ldots \lambda_{k\mathcal{K}}^{\mathbb{Q}} \right]_{\mathcal{K} \times 1}^{\mathrm{T}} ,$$

(3.22)

so that the nth element of $\tilde{V}_m^l$ (for $l = 1, \ldots, \mathcal{K}$) is given by the linear interpolation defined in (3.17) and (3.18)

$$\left[\tilde{V}_m^l \right]_{n^{th} \ element} = \mathcal{I}_{n,k,l} \left(V_m^l \right) .$$

When a Dirichlet condition is imposed at $S = S_{max}$, the last row of (3.21) is modified to

$$\begin{cases} \left[I - \theta M^k \right]_{\mathcal{N}^{th} \ row} & = [0 \ 0 \ldots 0 \ 1] , \\ \vec{u}_{RHS} & = [u_1 \ldots u_{\mathcal{N}-1} \ V_{*,\mathcal{N}}^k]^{\mathrm{T}}, \end{cases}$$

(3.23)

where $u_1 \ldots u_{\mathcal{N}}$ are the elements of the right hand side vector in (3.21) and $V_{*,\mathcal{N}}^k$ is the imposed value as the last element $(u_{\mathcal{N}})$.

The option values for each regime can be found by employing the fixed point-policy iteration of Algorithm 3.1 at each time step. Kennedy [23] and D'Halluin *et al.* [12] proved that the fixed point iteration scheme is globally convergent.

3.6 American Options

In this section, we extend our numerical scheme to various policy iteration methods in pricing American options under regime switching. While having the same structure as European options, American options differ in their giving the holder the right to exercise the option at anytime before the expiry to receive the payoff. The amount of

---

Algorithm 3.1 Fixed Point-Policy Iteration Method for European options (applied in each time step)

for $k = 1, \ldots, \mathcal{K}$

$\quad \left[I - \theta M^k\right] V^k_{m+1} = \left[I + (1-\theta)M^k\right] V^k_m + (1-\theta)\Delta\tau\Xi(V^k_m) + \theta\Delta\tau\Xi(V^k_{m+1})$

```
    for k = 1 to K do
```

$$\left(V^k_{m+1}\right)^{(0)} = V^k_m$$

```
        /* Initial guesses used in the first iteration (0)
            are the options values from the previous time step (m),
            except for Dirichlet nodes */

    end for
    j = 0 /* initialize counter for iteration */
    while ERROR > tolerance /* iteration loop */

        for k = 1 to K do /* regime loop */
            SOLVE
```

$$\left[I - \theta M^k\right] \left(V^k_{m+1}\right)^{(j+1)} = \left[I + (1-\theta)M^k\right] V^k_m + (1-\theta)\Delta\tau\Xi(V^k_m)$$
$$+ \theta\Delta\tau\Xi\left(\left(V^k_{m+1}\right)^{(j)}\right)$$

```
        end for          /* regime loop */
```
$$\text{ERROR} = \max_k \left\{ \max_n \left(\frac{\left|V^{k,j+1}_{m+1,n} - V^{k,j}_{m+1.n}\right|}{\max\left(1, \left|V^{k,j}_{m+1,n}\right|, \left|V^k_{m,n}\right|\right)} \right) \right\}$$
```
        j = j + 1

    end while /* iteration loop */
    TERMINAL ITERATE GIVES V^k_{m+1} FOR k = 1, ..., K
```

---

payoff depends on the current value of the underlying asset and a fixed strike price. The American option pricing problem is commonly expressed as a linear complementarity problem (LCP) which can be extended to the regime-switching model:

$$\begin{cases} (\partial_\tau - \mathcal{L} - \mathcal{J})V^k(\tau, S) & \geq 0 \\ V^k - V^k_* & \geq 0 \\ (V^k - V^k_*)(\partial_\tau V^k - \mathcal{L}\left[V^k\right] - \mathcal{J}\left[V^k\right]) & = 0, \ k = 1, \ldots, \mathcal{K}. \end{cases} \tag{3.24}$$

where V_*^k denotes the payoff received upon exercise in regime k. From (3.8), $\mathcal{L}$ and $\mathcal{J}$ operators are given by

$$\mathcal{L}\left[V^k\right] = \frac{1}{2}(\sigma^k)^2 S^2 V_{SS}^k + (r - \tilde{\eta}^k)SV_S^k - \left(r - \lambda^{kk}\right)V^k, \tag{3.25}$$

$$\mathcal{J}\left[V^k\right] = \sum_{l=1, l\neq k}^{\mathcal{K}} \lambda^{kl}V^l(S\bar{\eta}^{kl}), \ k = 1,\ldots,\mathcal{K}, \tag{3.26}$$

where V_S^k and V_{SS}^k are the first and second partial derivatives of the option value in regime k, with respect to S.

3.6.1   Penalty Method

The LCP problem (4.18) can be replaced by the penalty method so that

$$(\partial_\tau - \mathcal{L} - \mathcal{J})V^k(\tau, S) + P(V^k)(\tau, S) = 0, \tag{3.27}$$

where $P(v^k)(\tau, S) = \max_{\varphi \in \{0,1\}} \left[\varphi \frac{(V_*^k - V^k)}{\varepsilon}\right]$ is the penalty function and $\varepsilon \to 0$ is a penalty parameter.

The penalty method has been widely used since it was originally introduced in [16] for pricing American options. We assume the diagonal matrix $\bar{P}^k$ for regime k is given by

$$\begin{aligned}
\bar{P}^k(V_{m+1}^k)_{nn} &= \frac{\varphi_{m+1,n}^k}{\varepsilon} \quad , \\
\bar{P}^k(V_{m+1}^k)_{nq} &= 0 \quad ; \ \text{if } n \neq q,
\end{aligned} \tag{3.28}$$

where

$$\varphi_{m+1,n}^k \in \arg\max_{\varphi \in \{0,1\}} \left\{\frac{\varphi}{\varepsilon}(V_{m+1,n}^k - V_{*,n}^k)\right\}. \tag{3.29}$$

The matrix-form discrete equations (3.21) for American options can be rewritten as

28

$$\left[I - \theta M^k + \bar{P}^k(V_{m+1}^k)\right] V_{m+1}^k = \left[I + (1-\theta)M^k\right] V_m^k + (1-\theta)\Delta\tau\Xi(V_m^k) \qquad (3.30)$$

$$+ \theta\Delta\tau\Xi(V_{m+1}^k) + [\bar{P}^k(V_{m+1}^k)]V_*^k,$$

$$V_{m+1,\mathcal{N}}^k = \left[V_*^k\right]_{\mathcal{N}}; \text{ imposed at } S = S_{max} \qquad (3.31)$$

where the Dirichlet condition (the payoff) is imposed at $S = S_{max}$ using similar modifications as (3.23).

3.6.2 Direct Control Method

Equation (4.18) can be rewritten in control form [4]

$$\max_{\varphi \in \{0,1\}} \left[\Omega\varphi(V_*^k - V^k) - (1-\varphi)\left(\partial_\tau V^k - \mathcal{L}\left[V^k\right] - \mathcal{J}\left[V^k\right]\right)\right] = 0, \qquad (3.32)$$

where a scaling factor (Ω) is introduced into equation (3.32) since the two terms in the $\max(\cdot)$ expression have different units [20].

29

Discretizing equation (3.32), using an implicit method similar to (3.16), gives

$$\left[(1-\varphi_{m+1,n}^k)\left(1+\theta\Delta\tau(\alpha_n^k+\beta_n^k+r-\lambda_{kk}^{\mathbb{Q}})\right)+\Omega\Delta\tau\varphi_{m+1,n}^k\right]V_{m+1,n}^k \qquad (3.33)$$

$$-(1-\varphi_{m+1,n}^k)\theta\Delta\tau\left[\alpha_n^kV_{m+1,n-1}^k-\beta_n^kV_{m+1,n+1}^k\right]$$

$$=(1-\varphi_{m+1,n}^k)\left[1-(1-\theta)\Delta\tau(\alpha_n^k+\beta_n^k+r-\lambda_{kk}^{\mathbb{Q}})\right]V_{m,n}^k$$

$$+(1-\varphi_{m+1,n}^k)(1-\theta)\Delta\tau\left[\alpha_n^kV_{m,n-1}^k+\beta_n^kV_{m,n+1}^k\right]$$

$$+(1-\varphi_{m+1,n}^k)(1-\theta)\Delta\tau\sum_{l=1,l\neq k}^{\mathcal{K}}\lambda_{kl}^{\mathbb{Q}}\mathcal{I}_{n,k,l}\left(V_m^l\right)$$

$$+(1-\varphi_{m+1,n}^k)\theta\Delta\tau\sum_{l=1,l\neq k}^{\mathcal{K}}\lambda_{kl}^{\mathbb{Q}}\mathcal{I}_{n,k,l}\left(V_{m+1}^l\right)$$

$$+\Omega\Delta\tau\varphi_{m+1,n}^kV_{*,n}^k$$

where

$$\varphi_{m+1,n}^k\in\arg\max\{\Omega\varphi(V_{*,n}^k-V_{m+1,n}^k)-(1-\varphi)(\frac{V_{m+1,n}^k-V_{m,n}^k}{\Delta\tau} \qquad (3.34)$$

$$-\theta(\mathcal{L}V_{m+1,n}^k+\mathcal{J}V_{m,n-1}^k)-(1-\theta)(\mathcal{L}V_{m,n}^k+\mathcal{J}V_{m,n}^k))\}$$

with the discretized form of $\mathcal{L}$ and $\mathcal{J}$ operators defined as

$$\mathcal{L}V_{m,n}^k=\alpha_n^kV_{m,n-1}^k+\beta_n^kV_{m,n+1}^k-(\alpha_n^k+\beta_n^k+r-\lambda_{kk}^{\mathbb{Q}})V_{m,n}^k \qquad (3.35)$$

$$\mathcal{J}V_{m,n}^k=\sum_{l=1,l\neq k}^{\mathcal{K}}\lambda_{kl}^{\mathbb{Q}}\mathcal{I}_{n,k,l}\left(V_m^l\right) \qquad (3.36)$$

The matrix-form discrete equations(3.33) can be rewritten as

$$\left[\left(I - \phi_{m+1}^k\right)\left(I - \theta M^k\right) + \Omega\Delta\tau\phi_{m+1}^k\right]V_{m+1}^k = \left(I - \phi_{m+1}^k\right)\left[I + (1-\theta)M^k\right]V_m^k \qquad (3.37)$$

$$+ \left(I - \phi_{m+1}^k\right)\left[(1-\theta)\Delta\tau\Xi(V_m^k) + \theta\Delta\tau\Xi(V_{m+1}^k)\right]$$

$$+ \phi_{m+1}^k\Omega\Delta\tau V_*^k,$$

$$V_{m+1,\mathcal{N}}^k = \left[V_*^k\right]_{\mathcal{N}}; \text{ imposed at } S = S_{max} \qquad (3.38)$$

where $\phi_{m+1}^k = \left[\varphi_{m+1,1}^k, \ldots, \varphi_{m+1,\mathcal{N}}^k\right]^{\mathrm{T}}$ and the Dirichlet condition (the payoff) is imposed at $S = S_{max}$ using similar modifications as (3.23).

3.6.3   General Form of the Discretized Equations

For both the penalty and direct control methods, each timestep requires the solution of nonlinear equations. In these cases, the general form of the nonlinear equations is given by

$$\mathcal{A}^*(Q)U = \mathcal{C}(Q) \qquad (3.39)$$

$$\text{with } Q_q = \arg\max_{Q\in Z}\left[-\mathcal{A}^*(Q)U + \mathcal{C}(Q)\right]_q$$

where $\mathcal{A}^*(Q) = \mathcal{A}(Q) - \mathcal{B}(Q)$ is of size $\mathcal{KN} \times \mathcal{KN}$ and $U, \mathcal{C}$ are vectors of size $\mathcal{KN}$ in which $\mathcal{A}^*$ and $\mathcal{C}$ denote the coefficients of the associated linear systems with Q_q is the control for the qth node. Specifically, $\mathcal{A}(Q)$ provides coupled nodes within the same regime while $\mathcal{B}(Q)$ contains coupled nodes which belong to different regimes. Now, let U, the vector of option values in the $(m+1)^{th}$ timestep for all regimes $(1\ldots\mathcal{K})$, and $\mathcal{C}$,

the vector of controls, be represented by

$$U = [V_{m+1,1}^1, \ldots V_{m+1,\mathcal{N}}^1, \ldots, V_{m+1,1}^{\mathcal{K}}, \ldots, V_{m+1,\mathcal{N}}^{\mathcal{K}}]^{\mathrm{T}} \tag{3.40}$$

$$Q = [\varphi_{m+1,1}^1, \ldots \varphi_{m+1,\mathcal{N}}^1, \ldots, \varphi_{m+1,1}^{\mathcal{K}}, \ldots, \varphi_{m+1,\mathcal{N}}^{\mathcal{K}}]^{\mathrm{T}}.$$

Furthermore, we define matrices $\Gamma(V_m)$, ϕ_{m+1}, M as

$$\Gamma(V_m) = \left[\Xi(V_m^1)^{\mathrm{T}}, \ldots, \Xi(V_m^{\mathcal{K}})^{\mathrm{T}} \right]^{\mathrm{T}}$$

$$\phi_{m+1} = \mathrm{diag}(Q)$$

$$M = \mathrm{diag}(M^1, \ldots, M^{\mathcal{K}}),$$

where V_m, as defined in (3.15), is the vector of known option values from the mth timestep for all regimes $(1 \ldots \mathcal{K})$, $\Gamma(V_m)$ is the vector of regime-interpolated coupling terms for all regimes, ϕ_{m+1} is a diagonal matrix with elements of Q on the main diagonal, and M is a block-diagonal matrix with the k-th block on its diagonal containing matrix M^k.

Penalty Method

The discretized equations (3.30) can be written in terms of matrices $\mathcal{A}$, $\mathcal{B}$ and vector $\mathcal{C}$ given by

$$\mathcal{A}(Q)U = \mathcal{A}U = [(I - \theta M)] U + \left[\bar{P}(V_{m+1}) \right] U \tag{3.41}$$

$$\mathcal{B}(Q)U = \mathcal{B}U = \theta \Delta \tau \Gamma(U)$$

$$\mathcal{C}(Q) = \mathcal{C} = [I + (1 - \theta)M] V_m + \left[\bar{P}(V_{m+1}) \right] V_*$$

$$+ \left[(1 - \theta)\Delta \tau \Gamma(V_m) \right].$$

We impose a Dirichlet condition at $S = S_{max}$ for each regime (k). In terms of $\mathcal{A}$, $\mathcal{B}$ and vector $\mathcal{C}$, equation (3.42) is modified to

$$[\mathcal{A}U]_q = V^k_{m+1,\mathcal{N}}; \ [\mathcal{B}U]_q = 0; \ [\mathcal{C}]_q = \left[V^k_*\right]_{\mathcal{N}} \tag{3.42}$$

where $q = (k-1)\mathcal{N} + \mathcal{N} = k\mathcal{N}$; $\forall k \in \{1, \ldots, \mathcal{K}\}$ are all nodes corresponding to the imposed Dirichlet condition.

Direct Control

The discretized equations (3.30) can be written in terms of matrices $\mathcal{A}$, $\mathcal{B}$ and vector $\mathcal{C}$ given by

$$\mathcal{A}(Q)U = \mathcal{A}U = \left[(I - \phi_{m+1})(I - \theta M)\right]U + \left[\Omega\Delta\tau\phi_{m+1}\right]U \tag{3.43}$$
$$\mathcal{B}(Q)U = \mathcal{B}U = (I - \phi_{m+1})\theta\Delta\tau\Gamma(U)$$
$$\mathcal{C}(Q) = \mathcal{C} = (I - \phi_{m+1})\left[I + (1-\theta)M\right]V_m + \phi^k_{m+1}\Omega\Delta\tau V_*$$
$$+ (I - \phi_{m+1})\left[(1-\theta)\Delta\tau\Gamma(V_m)\right]$$

The same definitions as (3.42) can be used for the Dirichlet condition imposed at $S = S_{max}$.

3.6.4 Solution of the Discretized Equations

We investigate three approaches to solve equation (3.39) at each timestep, policy iteration, fixed point-policy iteration, and local policy iteration methods. Several techniques will be considered for solving the linear system at each iteration.

Algorithm 3.2 Policy Iteration Method for American Options
```
    U⁰ =Initial solution vector of size 𝒦𝒩
    for j = 0,1,2,... until converge do

        /* policy improvement: */
        Determine Qⱼ_q = arg max {−𝒜*(Q)Uʲ + 𝒞(Q)}_q
                         Q_q∈Z
        Qʲ = [Qʲ₁,...,Qʲ_𝒦𝒩]

        /* policy evaluation: */
        Solve 𝒜*(Qʲ)Uʲ⁺¹ = 𝒞(Qʲ)

        if j > 0 and max (Uⱼ⁺¹_q − Uⱼ_q)/max[scale,|Uⱼ⁺¹_q|] < tolerance then
                  q
            exit from the iteration
        end if

    end for
```

3.6.4.1 Policy Iteration Method

The policy iteration algorithm, or Howard's algorithm, is a standard method for solving dynamic programming problems. Given in Algorithm 3.2, the solution U is computed through a sequence of trial values (U^j) and policies (Q^j) under an alternating sequence of policy improvement and policy evaluation steps. The alternating process is recognized by separating the maximum operator from the linear system. Various techniques are introduced for solving the linear system

$$\left[\mathcal{A}(Q^j) - \mathcal{B}(Q^j)\right] U^{j+1} = \mathcal{C}(Q^j). \tag{3.44}$$

A direct solution method, while incorporating a minimum degree ordering for the sparse matrix $\mathcal{A}^*(Q^k)$, can be used. An iterative sparse solver and a simple iteration method are the other alternatives for solving the linear system.

It can be proved that policy iteration converges unconditionally for both the penalty (3.30) and direct control (3.37) discretizations [20].

Algorithm 3.3 Simple Iteration Method

```
    /* policy evaluation step: */
    (U^{j+1})^0 = U^j /* Initial solution vector for U^{j+1} */
    for m = 0, 1, 2, ... until converge do
```

$$\text{Solve } \left[\mathcal{A}(Q^j)\right] (U^{j+1})^{m+1} = \mathcal{B}(Q^j) (U^{j+1})^m + \mathcal{C}(Q^j)$$

$$\text{if } m > 0 \text{ and } \max_q \frac{\left(U_q^{j+1}\right)^{m+1} - \left(U_q^{j+1}\right)^m}{\max\left[scale, |\left(U_q^{j+1}\right)^{m+1}|\right]} < tolerance \text{ then}$$

```
            exit from the simple iteration

        end if

    end for
```

Simple Iteration Method

The linear system $\left[\mathcal{A}(Q^j) - \mathcal{B}(Q^j)\right] U^{j+1} = \mathcal{C}(Q^j)$ can be solved by employing a simple iteration. If $(U^{j+1})^m$ is the mth estimate for U^{j+1}, then

$$\left[\mathcal{A}(Q^j)\right] \left(U^{j+1}\right)^{m+1} = \mathcal{B}(Q^j) \left(U^{j+1}\right)^m + \mathcal{C}(Q^j) \tag{3.45}$$

where the initial guess for U^{j+1} is $(U^{j+1})^0 = U^j$. Algorithm 3.3 provides a simple iteration approach for the policy evaluation step in Algorithm 3.2 with a tolerance of 10^{-8}. The simple iteration will converge if $\|\mathcal{A}(Q^j)^{-1}\mathcal{B}(Q^j)\|_\infty < 1$.

Direct Solution Method (Minimum degree reordering)

We assemble the linear system (3.44) into a large sparse matrix and carry out a direct solution, using approximate minimum degree ordering [11], for the regime coupling terms. Each iteration requires the solution of the non-symmetric sparse matrix $(\mathcal{A} - \mathcal{B})$. The regime coupling terms in matrix $\mathcal{B}$ add nonzero entries into the incidence matrix with a block tridiagonal structure. We use an approximate minimum degree ordering based on the structure of the symmetrized matrix $((\mathcal{A} - \mathcal{B}) + (\mathcal{A} - \mathcal{B})^\mathsf{T})$. However, the actual symbolic factorization is carried out using the structure of the original matrix

$(\mathcal{A} - \mathcal{B})$.

GMRES-ILU Solver

We use a preconditioned GMRES technique [28, 15] for solving the linear system (3.44). An incomplete factorization based on zero level of fill (ILU(0)), which allows no fill-in, is incorporated. The convergence criteria is based on l_2 residual reduction[1] with a tolerance of 10^{-8}.

Algorithm 3.4 Fixed Point-Policy Iteration for American Options

---

$U^0 =$Initial solution vector of size $\mathcal{KM}$
for $j = 0, 1, 2, \ldots$ until converge do

  1. Determine

$$Q_q^j = \arg\max_{Q_q \in Z} \left\{ -\left[\mathcal{A}(Q) - \mathcal{B}(Q)\right] U^j + \mathcal{C}(Q) \right\}_q ;\ q = 1 \ldots \mathcal{KM}$$

$$Q^j = \left[Q_1^j, \ldots, Q_{\mathcal{KM}}^j \right]$$

  Solve $\mathcal{A}(Q^j)U^{j+1} = \mathcal{B}(Q^j)U^j + \mathcal{C}(Q^j)$

  if $j > 0$ and $\max \dfrac{U_q^{j+1} - U_q^{j+1}}{\max\left[scale, |U_q^{j+1}|\right]} < tolerance$ then quit

end for

3.6.4.2   Fixed Point-Policy Iteration Method

Using simple iteration for solving the linear system in the policy evaluation step leads to a double nested iteration algorithm. This, however, can be performed with only a single iteration at each nonlinear iterate. In this case, the policy iteration is replaced with a fixed point-policy iteration as suggested in [19]. It can be proved [20] that the fixed point-policy iteration, as described in Algorithm 3.4, is unconditionally convergent for the penalty (3.30) discretization, and converges for the direct control (3.37)

---

[1]The current rms residual is reduced to less than a user-specified fraction of the initial residual ($\frac{\|r^j\|_2}{\|r^0\|_2} < tol$)

discretization if $\Omega > \theta \cdot \hat{\lambda}$ where $\hat{\lambda} = \max_{k}\left(-\lambda_{kk}\right)$.

3.6.4.3   Local Policy Iteration Method

The nonlinear equations (3.39) can be solved by lagging the regime coupling terms and solving the American Linear Complementarity Problem (LCP) at each iteration [20]. With the regime coupling terms $(\mathcal{B}U^j)$ lagged one iteration, a local policy iteration is formulated in Algorithm 3.5. The solution of the nonlinear local control problem for the discrete equations appearing in the local policy step of Algorithm 3.5 can be obtained by either the penalty or direct control method. For both (3.30) and (3.37) equations, the local policy iteration converges at the rate [20]

$$\frac{\|E^{j+1}\|_\infty}{\|E^j\|_\infty} \leq \frac{\theta\hat{\lambda}\triangle\tau}{1+\theta(r+\hat{\lambda})}, \tag{3.46}$$

where $\hat{\lambda} = \max_{k}\left(-\lambda_{kk}\right)$, $E^j = U^j - U$, and U is the solution to (3.39).

Algorithm 3.5 Local Policy Iteration for American Options

$U^0 =$`Initial solution vector of size` $\mathcal{KM}$
`for` $j = 0, 1, 2, \ldots$ `until converge do`

　　`/* local policy */`
　　`Solve` $\max_{Q \in Z}\left\{-\mathcal{A}(Q)U^{j+1} + \mathcal{B}(Q)U^j + \mathcal{C}(Q)\right\} = 0$

　　`if` $j > 0$ `and` $\max\frac{U^{j+1}-U^{j+1}}{\max[scale, |U^{j+1}|]} < tolerance$ `then`
　　　　`exit from the iteration`
　　`end if`

`end for`

3.7   Numerical Experiments

We price an American put option in a three-state regime-switching model where the underlying jumps in each regime shift. The market is from [23], where the stock follows

37

a Geometric Brownian Motion model within each state. The interest rate is $r = 0.02$, with regime-dependent volatilities $\vec{\sigma} = [0.0955, 0.0644, 0.0241]$. The rate matrix of risk adjusted intensities is

$$\Lambda^{\mathbb{Q}} = \begin{bmatrix} -3.5613 & 0.2405 & 3.3208 \\ 1.1279 & -1.2008 & 0.0729 \\ 2.9882 & 0.2025 & -3.1907 \end{bmatrix}, \qquad (3.47)$$

with jump amplitudes

$$\eta = \begin{bmatrix} 1 & 0.9095 & 1.0279 \\ 1.2502 & 1 & 1.6512 \\ 0.9693 & 0.7732 & 1 \end{bmatrix}, \qquad (3.48)$$

where the entry placed in (k, l) corresponds to the transition from regime k to l.

We consider an American put option with $T = 0.5$ and a strike of $K = 100\$$ which is priced at $S = 100\$$. The American option pricing problem in (4.18) is solved numerically using Policy Iteration, Fixed Point-Policy Iteration, and Local Policy Iteration combined with both the penalty and direct control [4] methods. The penalty parameter, scaling factor, and convergence tolerances for inner and outer iterations are set to $\varepsilon = 10^{-6}\Delta\tau$, $\Omega = 1/\varepsilon$, $tol = 10^{-8}$, respectively.

3.7.1 Convergence and Computations

Policy Iteration Method

Policy iteration method, as described in Algorithm 3.2, is combined with the penalty or direct control discretizations for solving the American LCP problem. The solution of the linear system (3.44), however, is obtained using a simple iteration, direct solution or

a PCG-like iterative solver (GMRES-ILU(0)). Examples of incorporating these various techniques are shown in Tables 3.1 and 3.2 combined with the penalty approach, and Tables 3.3 and 3.4 combined with the direct control approach. Various timestepping for consecutive refinements of the grid is considered for all cases.

It can be observed that in terms of the convergence of the discretization of the LCP problem, quadratic convergence is not guaranteed even with a variable timestepping method, and the results for different regimes are not consistent. While the rate of convergence is oscillatory within each regime, different regimes are inconsistent in terms of the convergence rates. The oscillation and inconsistency observed in the convergence rates can be due to the interpolated option values after a jump occurs. For those spot prices near the strike, or even far from that when the jump amplitude is large, a jump may have a significant effect on the option values. In the absence of jump terms (section 3.7.3), both the oscillation and inconsistency are expected to disappear.

Both the penalty and direct control formulations have similar convergence behaviors. Among various techniques, the simple iteration is more efficient than both the direct and GMRES-ILU(0) solution methods. For instance, according to Tables 3.1 and 3.2, while computing the option values takes 126 seconds for a grid of size $\mathcal{N} = 3200$ in the simple iteration method, 12142 and 231 seconds are the costs associated with the direct and GMRES-ILU(0) solution, respectively. Furthermore, as can be seen in Tables 3.2 and 3.4, there is a significant difference between the amount of work needed for the direct solution and other methods. Similar to the convergence ratio definition, we define a relative change in the amount of work (computations) for the i-th refinement represented in the last column of the aforementioned tables so that

$$Rate = \frac{t_i - t_{i-1}}{t_{i-1} - t_{i-2}}, \qquad (3.49)$$

where t_i is the amount of CPU time spent for the i-th refinement. While this rate is

stable and around 4 for other methods, an increasing relative change in the amount of work is observed for the direct method. Specifically, the last refinement in Table 3.2 implies that the extra amount of computation is 12.41 times more than the previous refinement which makes the direct method very expensive.

Policy Iteration Method (Penalty / Simple Iteration)

| $\mathcal{N}$ | Regime 1 | | | Regime 2 | | | Regime 3 | | | Time | |
	Value	Change	Ratio	Value	Change	Ratio	Value	Change	Ratio	Time (s)	Rate**
100	3.163237697			7.87620801			3.038006453			0.2	
200	3.140096408	0.02314129		7.871012198	0.00519581		2.991042676	0.04696378		0.6	
400	3.139543876	0.00055253	41.88	7.870074165	0.00093803	5.54	2.989786522	0.00125615	37.39	2.2	3.23
800	3.139542917	0.00000096	576.2	7.869812031	0.00026213	3.58	2.989811831	0.00002531	49.63	7.7	3.66
1600	3.139542811	0.00000011	9.1	7.869726457	0.00008557	3.06	2.989818156	0.00000632	4	30.9	4.16
3200	3.139542838	0.00000003	3.98	7.869715397	0.00001106	7.74	2.989819796	0.00000164	3.86	126.7	4.14
	** Rate ≡ Relative Change in Computations										

Table 3.1: *Pricing of a half-year American put option in the three-state market from [23] with jumps and variable timestepping for consecutive refinements of the grid. Penalty American and Simple Iteration are used for the outer and inner loops, respectively. The order of convergence is sometimes oscillatory (regime 1 and 2)*

Policy Iteration Method (Penalty / Direct Solution - GMRES-ILU(0))

| $\mathcal{N}$ | Regime 1 | | Regime 2 | | Regime 3 | | Time | | | |
| | | | | | | | Direct Solution | | GMRES-ILU(0) | |
	Value	Ratio*	Value	Ratio	Value	Ratio	Time (s)	Rate**	Time (s)	Rate
100	3.163237699		7.876208011		3.038006455		0.2		0.2	
200	3.140096408		7.871012198		2.991042676		1.3		0.8	
400	3.139543877	41.88	7.870074165	5.54	2.989786523	37.39	6.8	5.25	3.4	4.08
800	3.139542918	576.2	7.869812031	3.58	2.989811832	49.63	71.4	11.72	14	4.21
1600	3.139542812	9.02	7.869726457	3.06	2.989818156	4	971	13.93	57.5	4.07
3200	3.139542838	4.04	7.869715397	7.74	2.989819796	3.86	12142	12.41	231	4.01
	* Ratio ≡ Convergence Ratio									
	** Rate ≡ Relative Change in Computations									

Table 3.2: *Pricing of a half-year American put option in the three-state market from [23] with jumps and variable timestepping for consecutive refinements of the grid. The outer loop is the penalty American iteration and the inner layer is either the GMRES-ILU(0) or direct-solved regime layer. The order of convergence is sometimes oscillatory (regime 1 and 2)*

Policy Iteration Method (Direct Control / Simple Iteration)

$\mathcal{N}$	Regime 1			Regime 2			Regime 3			Time	
	Value	Change	Ratio	Value	Change	Ratio	Value	Change	Ratio	Time (s)	Rate
100	3.163237699			7.87620801			3.038006454			0.2	
200	3.140096409	0.02314129		7.871012198	0.00519581		2.991042677	0.04696378		0.7	
400	3.139543876	0.00055253	41.88	7.870074165	0.00093803	5.54	2.989786523	0.00125615	37.39	2.4	3.36
800	3.139542917	0.00000096	576	7.869812031	0.00026213	3.58	2.989811832	0.00002531	49.63	8.5	3.66
1600	3.139542812	0.00000011	9.09	7.869726457	0.00008557	3.06	2.989818156	0.00000632	4	34.8	4.28
3200	3.139542838	0.00000003	4.01	7.869715397	0.00001106	7.74	2.989819796	0.00000164	3.86	143.8	4.14

Table 3.3: *Pricing of a half-year American put option in the three-state market from [23] with jumps and variable timestepping for consecutive refinements of the grid. Direct Control and Simple Iteration are used for the outer and inner loops, respectively. The order of convergence is sometimes oscillatory (regime 1 and 2)*

Policy Iteration Method (Direct Control / Direct Solution - GMRES-ILU(0))

$\mathcal{N}$	Regime 1		Regime 2		Regime 3		Time			
							Direct Solution		GMRES-ILU(0)	
	Value	Ratio*	Value	Ratio	Value	Ratio	Time (s)	Rate**	Time (s)	Rate
100	3.163237701		7.876208011		3.038006456		0.3		0.3	
200	3.140096409		7.871012198		2.991042677		1.4		1.1	
400	3.139543876	41.88	7.870074165	5.54	2.989786524	37.39	7.6	5.30	3.9	3.59
800	3.139542918	576.7	7.869812031	3.58	2.989811833	49.63	74.4	10.76	16.1	4.28
1600	3.139542812	9	7.869726457	3.06	2.989818156	4	936	12.92	72.8	4.66
3200	3.139542838	4.06	7.869715397	7.74	2.989819796	3.86	13377	14.43	334	4.62

* Ratio ≡ Convergence Ratio

** Rate ≡ Relative Change in Computations

Table 3.4: *Pricing of a half-year American put option in the three-state market from [23] with jumps and variable timestepping for consecutive refinements of the grid. The outer loop is the direct control iteration and the inner layer is either the GMRES-ILU(0) or direct-solved regime layer. The order of convergence is sometimes oscillatory (regime 1 and 2)*

Fixed Point-Policy Iteration Method

Fixed point policy iteration uses a single iteration to solve the nonlinear problem.

Tables 3.5 and 3.6 provides convergence and computational cost results for the local

policy iteration method combined with the penalty and direct control approach. It can be observed that the computational costs compete with the outputs from the policy iteration method while a simple iteration technique (Tables 3.1, 3.3) is applied to the linear system.

Fixed Point Policy Iteration Method (Penalty)

| $\mathcal{N}$ | Regime 1 | | | Regime 2 | | | Regime 3 | | | Time | |
	Value	Change	Ratio	Value	Change	Ratio	Value	Change	Ratio	Time (s)	Rate
100	3.163237697			7.876208010			3.038006453			0.2	
200	3.140096408	0.02314129		7.871012198	0.00519581		2.991042676	0.04696378		0.6	
400	3.139543876	0.00055253	41.88	7.870074165	0.00093803	5.54	2.989786522	0.00125615	37.39	2.2	3.57
800	3.139542917	0.00000096	576	7.869812031	0.00026213	3.58	2.989811831	0.00002531	49.63	7.7	3.57
1600	3.139542811	0.00000011	9.12	7.869726457	0.00008557	3.06	2.989818156	0.00000632	4	31.3	4.35
3200	3.139542838	0.00000003	3.97	7.869715397	0.00001106	7.74	2.989819796	0.00000164	3.86	126.2	4.00

Table 3.5: *Pricing of a half-year American put option in the three-state market from [23] with jumps and variable timestepping for consecutive refinements of the grid. Penalty American is used for the outer iteration. The order of convergence is sometimes oscillatory (regime 1 and 2)*

Fixed Point Policy Iteration Method (Direct Control)

| $\mathcal{N}$ | Regime 1 | | | Regime 2 | | | Regime 3 | | | Time | |
	Value	Change	Ratio	Value	Change	Ratio	Value	Change	Ratio	Time (s)	Rate
100	3.163237699			7.87620801			3.038006454			0.2	
200	3.140096409	0.02314129		7.871012198	0.00519581		2.991042676	0.04696378		0.7	
400	3.139543876	0.00055253	41.88	7.870074165	0.00093803	5.54	2.989786523	0.00125615	37.39	2.4	3.45
800	3.139542917	0.00000096	576	7.869812031	0.00026213	3.58	2.989811831	0.00002531	49.63	8.9	3.85
1600	3.139542812	0.00000011	9.1	7.869726457	0.00008557	3.06	2.989818156	0.00000632	4	35.1	4.00
3200	3.139542838	0.00000003	3.99	7.869715397	0.00001106	7.74	2.989819796	0.00000164	3.86	141	4.00

Table 3.6: *Pricing of a half-year American put option in the three-state market from [23] with jumps and variable timestepping for consecutive refinements of the grid. Direct Control is used for the outer iteration. The order of convergence is sometimes oscillatory (regime 1 and 2)*

Local Policy Iteration Method

Local policy iteration method, as described in Algorithm 3.5, is combined with the penalty and direct control approaches for solving the local American problem. The convergence and computational cost results are provided in Tables 3.7 and 3.8. Compared to the fixed point policy iteration, the local policy iteration is not more efficient. While the last refinement of the experiment takes 126 seconds for the former in the penalty case, 152 seconds is required for the latter in the same case.

Local Policy Iteration Method (Penalty)

$\mathcal{N}$	Regime 1			Regime 2			Regime 3			Time	
	Value	Change	Ratio	Value	Change	Ratio	Value	Change	Ratio	Time (s)	Rate
100	3.163237699			7.876208011			3.038006455			0.2	
200	3.140096408	0.02314129		7.871012198	0.00519581		2.991042676	0.04696378		0.7	
400	3.139543877	0.00055253	41.88	7.870074165	0.00093803	5.54	2.989786523	0.00125615	37.39	2.3	3.23
800	3.139542918	0.00000096	576.2	7.869812031	0.00026213	3.58	2.989811832	0.00002531	49.63	8.6	3.85
1600	3.139542811	0.00000011	9.01	7.869726457	0.00008557	3.06	2.989818156	0.00000632	4.00	37.6	4.55
3200	3.139542838	0.00000003	4.03	7.869715397	0.00001106	7.74	2.989819796	0.00000164	3.86	152.6	4.00

Table 3.7: *Pricing of a half-year American put option in the three-state market from [23] with jumps and variable timestepping for consecutive refinements of the grid. Penalty American is used for the inner iteration. The order of convergence is sometimes oscillatory (regime 1 and 2)*

Local Policy Iteration Method (Direct Control)

$\mathcal{N}$	Regime 1			Regime 2			Regime 3			Time	
	Value	Change	Ratio	Value	Change	Ratio	Value	Change	Ratio	Time (s)	Rate
100	3.163237701			7.876208011			3.038006456			0.2	
200	3.140096409	0.02314129		7.871012198	0.00519581		2.991042677	0.04696378		0.7	
400	3.139543877	0.00055253	41.88	7.870074165	0.00093803	5.54	2.989786524	0.00125615	37.39	2.5	3.57
800	3.139542918	0.00000096	576	7.869812031	0.00026213	3.58	2.989811833	0.00002531	49.63	10.0	4.17
1600	3.139542812	0.00000011	9.02	7.869726457	0.00008557	3.06	2.989818156	0.00000632	4.00	40.9	4.17
3200	3.139542838	0.00000003	4.06	7.869715397	0.00001106	7.74	2.989819796	0.00000164	3.86	184.7	4.55

Table 3.8: *Pricing of a half-year American put option in the three-state market from [23] with jumps and variable timestepping for consecutive refinements of the grid. Direct Control is used for the inner iteration. The order of convergence is sometimes oscillatory (regime 1 and 2)*

3.7.2 Iteration Comparisons

We compare the performance of iterative algorithms 3.2, 3.4, and 3.5 combined with the penalty method for solving the LCP problem. For both the full and local policy iteration methods, the number of inner per outer iterations, inner iterations per timestep, and outer iterations per timestep are given in Table 3.9 for reasonable timesteps. We analyze these ratios with the number of outer iterations per timestep in the fixed point policy iteration.

When a simple iteration is used, 2.2 outer (penalty American) iterations with each two inner (regime coupling) iterations are observed. In the absence of inner iterations, a small increase (2.2 to 3) in the number of outer (penalty American) is required for the convergence of the fixed point method. The local policy iteration converges after three outer (regime coupling) iterations per timestep and 1.7 inner (penalty American) per outer iteration.

From a computational perspective, the first two methods (full policy and fixed point) require less work compared to the local policy method.

44

Ratios of Inner and Outer iterations

Method	Inner/Outer	Inner/Tstep	Outer/Tstep	Time (s)
Full Policy Iteration (Simple Iteration)	2	4.4	2.2	126.7
Fixed Point	N/A	N/A	3	126.2
Local Policy Iteration	1.7	5.1	3	152.6

Table 3.9:   *The average inner per outer iterations, inner per time-step, and outer per time-step when pricing of a half-year American put option in the three-state market from [23] with jumps and variable timestepping for consecutive refinements of the grid. The Penalty formulation is used.*

3.7.3   The No-jump Model

The 3-state market from [23] is assumed to have jumps, with jump amplitudes given in (3.48), due to each shift in regime. Having considered all other parameters unchanged, we recompute the numerical experiments for the model with no jump ($[\eta]_{ij} = 1$, $\forall i, j$). Table 3.10 gives results for the model with no jump when the outer penalty American iteration is accompanied by a direct-solve approach for the regime iteration. Unlike the original model from [23], we observe similar behaviour for the rate of convergence among all regimes. Significantly, contrary to the model with jumps allowed in each regime shift, quadratic convergence is achieved due to variable timestepping.

<p style="text-align:center">Direct Solution Method - No Jump</p>

$\mathcal{N}$	Regime 1			Regime 2			Regime 3			Time	
	Value	Change	Ratio	Value	Change	Ratio	Value	Change	Ratio	Time (s)	Rate
100	1.753928067			1.531024769			1.138502925			0.1	
200	1.756205946	0.00227788		1.533292054	0.00226729		1.142211095	0.00370817		0.2	
400	1.756794218	0.00058827	3.87	1.533870738	0.00057868	3.92	1.143165712	0.00095462	3.88	0.7	4.17
800	1.756944802	0.00015058	3.91	1.534017316	0.00014658	3.95	1.143409895	0.00024418	3.91	2.6	4.00
1600	1.756982758	0.00003796	3.97	1.534054239	0.00003692	3.97	1.143471664	0.00006177	3.95	10.9	4.17
3200	1.756992323	0.00000957	3.97	1.534063563	0.00000932	3.96	1.143487247	0.00001558	3.96	43.9	4.00

Table 3.10: *Pricing of a half-year American put option in the three-state market from [23](except that there is no jump between regimes) and variable timestepping for consecutive refinements of frequency-time grid. The outer loop is the penalty American iteration and the inner layer is the direct-solved regime layer. Quadratic convergence is observed due to variable timestepping and no jump between regimes.*

3.7.4 Direct Solution Sparsity Patterns

It is interesting to examine the sparsity pattern of the factors when using a direct method to solve the full policy iteration matrix. We assembled the linear system (3.21) for each regime into a large sparse matrix and carried out a direct solution, using minimum degree ordering. The coefficient matrix ($\mathcal{A}^* = \mathcal{A} - \mathcal{B}$) in (3.44) is a sparse matrix with the sparsity patterns shown in Figure 3.1 for the 3-state model from [23] with the grid of size $\mathcal{N} = 101$. The left graph is the sparse matrix ($\mathcal{A}^*$) with 2100 non-zero elements. The corresponding symmetrized and reordered matrices of the matrix ($\mathcal{A}^*$) are given in the middle and right graphs, respectively, with 2887 non-zero elements. Figure 3.2 shows sparsity patterns of the lower and upper triangular matrices from the LU decomposition of the linear system (3.21).There is still significant number of fill-in ($2219 + 2389 = 4608$) in the lower and upper triangular matrices.

Similarly, Figure 3.3 shows the sparsity patterns when there is no jump between regimes in the 3-state model from [23]. The left graph is the sparse matrix ($\mathcal{A}^*$) with 1503 non-zero elements. The corresponding symmetrized and reordered matrices of the
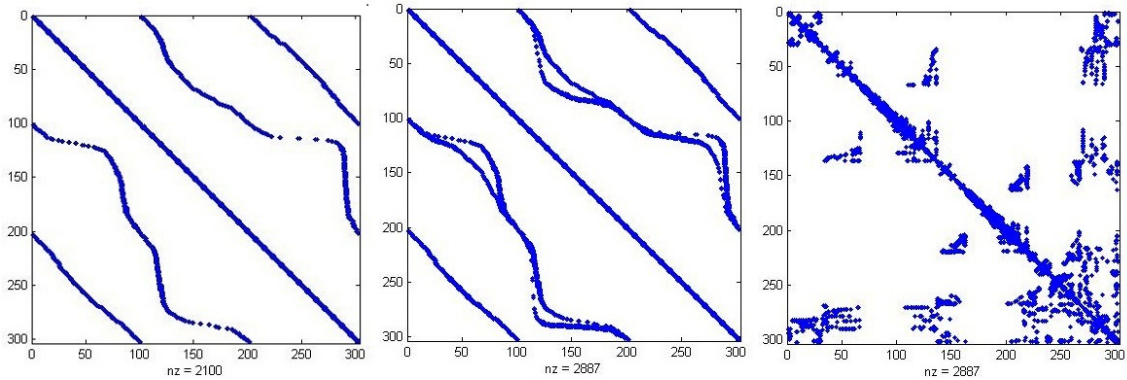
Figure 3.1: *Sparsity patterns of the coefficient matrix in the linear system (3.21) when assembled into a large sparse matrix (3$\mathcal{N}$ * 3$\mathcal{N}$, where $\mathcal{N}$ = 101) in the three-state market from [23]. The left graph is the sparse coefficient matrix with 2100 non-zero elements. Middle and right are symmetrized and reordered matrices, respectively, with 2887 non-zero elements.*
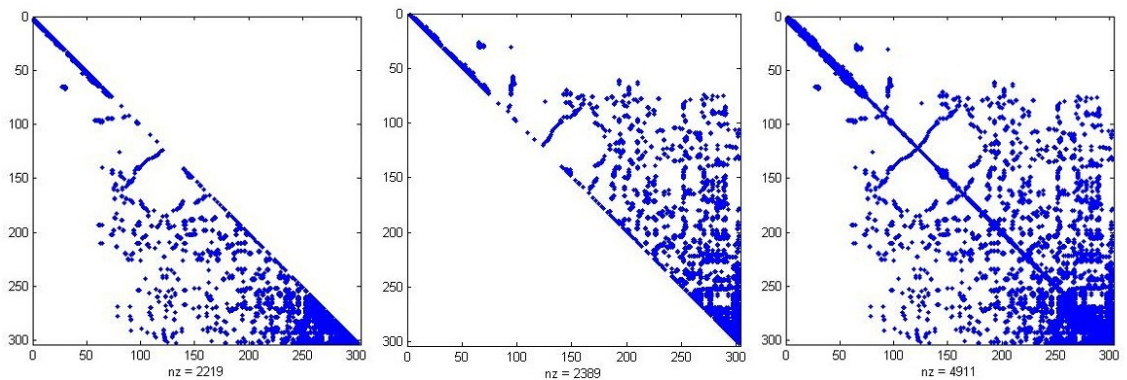
Figure 3.2: *Sparsity patterns of the lower and upper triangular matrices coming from the LU decomposition of the linear system (3.21) when assembled into a large sparse matrix (3$\mathcal{N}$ * 3$\mathcal{N}$, where $\mathcal{M}$ = 101) in the three-state market from [23] .*

matrix ($\mathcal{A}^*$) are given in the middle and right graphs, respectively, with 1509 non-zero elements. Figure 3.4 shows sparsity patterns of the lower and upper triangular matrices from the LU decomposition of the linear system (3.21). Compared to the original model, the model with no jump has better results in terms of the number of fill-in ($902 + 892 = 1794$ non-zero elements in the lower and upper triangular matrix). Furthermore, it can be observed from Table 3.10 that the no-jump model has a significant improvement in terms of the computational time cost ($74.6s$ vs $4871s$ for the original model when $\mathcal{N} = 3200$). This can be explained by the fact that matrix ($\mathcal{A}^* + (\mathcal{A}^*)^\mathsf{T}$) is a tridiagonal block matrix in the no-jump model which makes the reordering algorithm much faster.
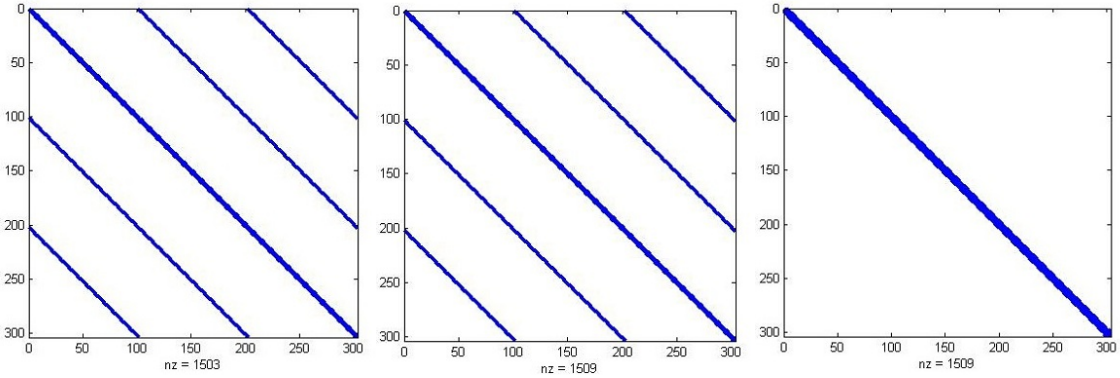
Figure 3.3: *Sparsity patterns of the coefficient matrix in the linear system (3.21) when assembled into a large sparse matrix (3$\mathcal{N}$ * 3$\mathcal{N}$, where $\mathcal{N} = 101$) in the three-state market from [23] (except that there is no jump between regimes). The left graph is the sparse coefficient matrix with 1503 non-zero elements. Middle and right are symmetrized and reordered matrices, respectively, with 1509 non-zero elements.*

In fact, it is easy to see how the reordered matrix for the no-jump case has a small amount of fill. Consider ordering the row and columns so that all variables associated with a single node (all regimes) are ordered consecutively. This results in a sparsity
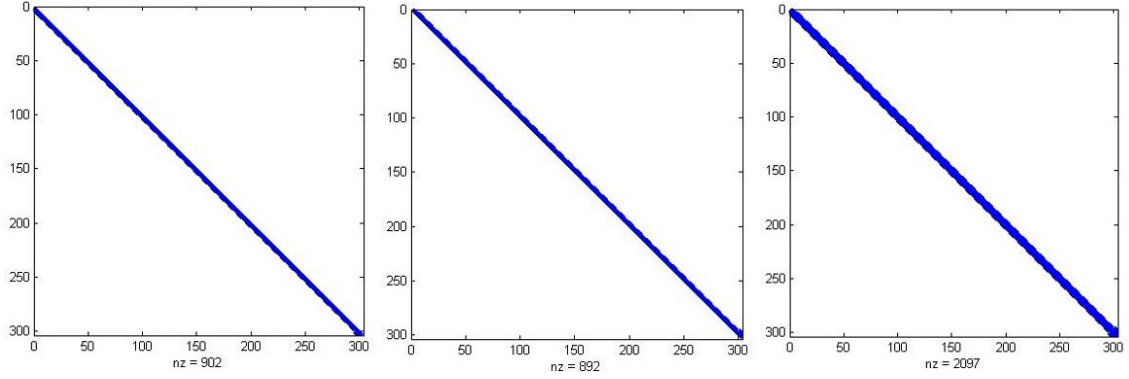
Figure 3.4: *Sparsity patterns of the lower and upper triangular matrices coming from the LU decomposition of the linear system (3.21) when assembled into a large sparse matrix (3$\mathcal{N}$ * 3$\mathcal{N}$, where $\mathcal{N} = 101$) in the three-state market from [23] (except that there is no jump between regimes).*

pattern

$$
\begin{bmatrix}
D_1 & U_1 & & & \cdots & & 0 \\
L_2 & D_2 & U_2 & & & & \\
& & \ddots & & & & \vdots \\
& & L_n & D_n & U_n & & \\
\vdots & & & & \ddots & & \\
& & & & L_{\mathcal{N}-1} & D_{\mathcal{N}-1} & U_{\mathcal{N}-1} \\
0 & & \cdots & & & L_{\mathcal{N}} & D_{\mathcal{N}}
\end{bmatrix}
\tag{3.50}
$$

where L_n, D_n, and U_n are square sub-matrices of the low, main and upper diagonal, respectively. The general form of these sub-matrices is given by

$$
L_n = \begin{bmatrix} l_{11} & 0 & 0 \\ 0 & l_{22} & 0 \\ 0 & 0 & l_{33} \end{bmatrix} ; \quad D_n = \begin{bmatrix} d_{11} & d_{12} & d_{13} \\ d_{21} & d_{22} & d_{23} \\ d_{31} & d_{32} & d_{33} \end{bmatrix} ; \quad U_n = \begin{bmatrix} u_{11} & 0 & 0 \\ 0 & u_{22} & 0 \\ 0 & 0 & u_{33} \end{bmatrix} , \quad n = 1 \ldots \mathcal{N},
$$

where l_{ij}, d_{ij}, and $u_{ij} \neq 0$; $i, j = 1, 2, 3$. Therefore, the sparsity pattern in (3.50) has $15 \times \mathcal{N} - 6$ nonzero elements which equals 1509 for $\mathcal{N} = 101$. Moreover, A rough

49

estimate of the total number of nonzeros in the LU factors is $7 \times 3 \times \mathcal{N}$ which equals 2100 for $\mathcal{N} = 101$. These results conform to the sparsity patterns shown in the right graphs of Figures 3.3 and 3.4.

Chapter 4

Fourier Space Time-stepping Method

4.1 Introduction

A Fourier transform can be applied to a system of option pricing PDEs to obtain a linear system of ordinary differential equations (ODEs). The Fourier Space Time-stepping algorithm (FST) considers the transformed PDEs with a time-stepping scheme in the frequency domain, in which the frequency domain prices are obtained by applying the discrete Fourier transform (DFT) to the spatial domain. In this chapter, the FST method for pricing path-dependent options is developed. The availability of an analytical Fourier method depends on the form of the option payoff and the linearity of the corresponding PDEs. For instance, the appearance of a nonlinear term in the American option pricing PDEs can not be resolved using an analytical Fourier method. Therefore, we approximate the sampled continuous frequency domain prices with the discrete Fourier transform of the option values and proceed with the time-stepping scheme by using an iterative FST algorithm in the frequency domain. The algorithm uses a single time step for pricing European-style options while multiple steps are required for American options.

4.2 Continuous Fourier Transformation of the PDEs

In Chapter 3, we derived the system of option pricing PDEs for a European option under a general $\mathcal{K}$-state regime-switching model [23] as

for $k = 1, \ldots, \mathcal{K}$:

$$
\begin{cases}
\dfrac{\partial V^k}{\partial t} + \frac{1}{2}(\sigma^k)^2 S^2 \dfrac{\partial^2 V^k}{\partial S^2} + (r - \tilde{\eta}^k) S \dfrac{\partial V^k}{\partial S} - rV^k + \sum_{l=1, l \neq k}^{\mathcal{K}} \lambda^{kl}(V^l(S\eta^{kl}) - V^k) = 0, \\
V^k(S, T) = V_*^k.
\end{cases}
$$

(4.1)

A logarithmic transformation converts the system of PDEs in (4.1) to a system of constant-coefficient PDEs. Therefore, if $x = \log(\frac{S}{S_0})$ and $j^{kl} = \log(\eta^{kl})$, and $v^{(k)}(t, \mathrm{x})$ denotes the discounted-adjusted and log-transformed price at time t, state k, and spot level x, the system of PDEs in (4.1) for pricing European options can be re-expressed as

$$
\begin{cases}
\dfrac{\partial v^k}{\partial t} + \frac{1}{2}(\sigma^i)^2 \dfrac{\partial^2 v^k}{\partial x^2} + (r - \tilde{\eta}^k - \frac{1}{2}(\sigma^k)^2) \dfrac{\partial v^k}{\partial x} - rv^k \\
\qquad\qquad\qquad + \sum_{l=1, l \neq k}^{\mathcal{K}} \lambda^{kl} \left(v^l(x + j^{kl}) - v^k \right) \quad = 0, \\
v^k(x, T) = v_*^k.
\end{cases}
$$

(4.2)

Applying a Fourier transform to the system of constant coefficient PDEs leads to a system of ODEs. Surkov [30] incorporated a $\mathcal{K}$-state continuous Markov chain into the joint stock price process model S(t) which follows a d-dimensional exponential Lévy process, and applied a Fourier transform to convert the PIDE into a system of ODEs. Given the same procedure for a regime-switching model with GBM process, we take Fourier transform of the system in (4.2). In this chapter, i represents $\sqrt{-1}$, and $\mathcal{F}[\cdot]$ denotes the continuous Fourier transform of the term in the brackets. Now, the following rules

$$
\mathcal{F}\left[\partial_x^n g\right](\omega) = i\omega \mathcal{F}\left[\partial_x^{n-1} g\right](\omega) = \cdots = (i\omega)^n \mathcal{F}[g](\omega),
$$

and

$$\mathcal{F}\left[g(x-a)\right](\omega) = e^{-ia\omega}\mathcal{F}\left[g(x)\right](\omega)$$

give us

$$
\begin{cases}
\dfrac{\partial F^k}{\partial t} + \tfrac{1}{2}(i\omega)^2(\sigma^k)^2 F^k + (i\omega)(r - \tilde{\eta}^k - \tfrac{1}{2}(\sigma^k)^2)F^k - rF^k \\
\qquad\qquad\qquad\qquad + \sum_{l=1,l\neq k}^{\mathcal{K}} \lambda^{kl}(e^{i\jmath^{kl}\omega}F^l - F^k) \;\; = 0, \\
F^k(T,\omega) = F_*^k,
\end{cases}
\tag{4.3}
$$

where $F^k(t,\omega) = \mathcal{F}\left[v^k\right](t,\omega)$ and $F_*^k = \mathcal{F}\left[v_*^k\right](T,\omega)$ in continuous time. From $\lambda^{kk} = -\sum_{l=1,l\neq k}^{\mathcal{K}} \lambda^{kl}$, we have

$$
\begin{cases}
\dfrac{\partial F^k}{\partial t} + \left(\lambda^{kk} + (i\omega)^2\tfrac{1}{2}(\sigma^k)^2 + (i\omega)(r - \tilde{\eta}^k - \tfrac{1}{2}(\sigma^k)^2) - r\right)F^k \\
\qquad\qquad\qquad\qquad\qquad + \sum_{l=1,l\neq k}^{\mathcal{K}} \lambda^{kl}e^{i\jmath^{kl}\omega}F^l \;\; = 0, \\
F^k(T,\omega) = F_*^k.
\end{cases}
\tag{4.4}
$$

We can also define a matrix form of equation (4.4). Let $\boldsymbol{\Psi}$ denote the matrix characteristic function with the following elements

$$
\langle\Psi(\omega)\rangle_{kl} =
\begin{cases}
\lambda^{kk} - \tfrac{1}{2}(\sigma^k)^2\omega^2 + i[(r - \tilde{\eta}^k - \tfrac{1}{2}(\sigma^k)^2)]\omega - r, & k = l \\
\lambda^{kl}e^{i\jmath^{kl}\omega}, & k \neq l
\end{cases}
\tag{4.5}
$$

For each specific ω, (4.4) can be displayed in a matrix form

$$
\begin{cases}
\dfrac{\partial F(t,\omega)}{\partial t} + \Psi(\omega)F(t,\omega) = 0 \\
F(T,\omega) = F_* \\
F = \left[F^1, F^2, \ldots, F^k, \ldots, F^{\mathcal{K}}\right]^{\mathrm{T}}, \;\; k=\text{regime number.}
\end{cases}
\tag{4.6}
$$

53

The coupled system of ODEs (4.6), expressed by the homogeneous matrix form, can be easily solved for the vector of transformed prices by

$$F(t, \omega) = \exp\{(T - t)\Psi(\omega)\}F_*(\omega), \tag{4.7}$$

where $\exp\{(T - t)\Psi(\omega)\}$ represents the complex matrix exponential. Option prices are then obtained by taking a reverse Fourier transform, in which a single step for European options and multiple steps for American option are required. For European options

$$v = \mathcal{F}^{-1}\left[e^{(T-t)\Psi(\omega)}F_*(\omega)\right], \tag{4.8}$$

where $v = \left[v^1, \ldots, v^\mathcal{K}\right]^{\mathbf{T}}$ is the vector of regime-dependent option values in the real space.

4.3   Numerical Solution

Since an explicit expression for the Fourier transform of the option payoff is not guaranteed, the system of ODEs obtained analytically in (4.6) cannot, necessarily, be solved analytically. Furthermore, path-dependent features such as early exercise of American options leads to a non-linear term in the corresponding PDE that cannot be treated using an analytical Fourier method. Therefore, we attempt to sample the continuous frequency domain prices using a finite number of points in the frequency domain and approximate it with a discrete Fourier transform (DFT) of the option value in the spatial domain. The DFT is computed efficiently using the fast Fourier transform (FFT) algorithm.

4.3.1   Grid Selection and Discretization of the Fourier Space

The numerical algorithm for the Fourier transform-based solution (4.8) requires one step for European and multiple steps for American options. We use the following notations

$$
\begin{aligned}
k & \quad \text{regime number} \quad (1,\dots,\mathcal{K}) \\
m & \quad \text{timestep index} \quad (1,\dots,\mathcal{M}) \\
n & \quad \text{asset node index} \quad (1,\dots,\mathcal{N}),
\end{aligned}
$$

to construct the spatial grid. Similar to Surkov [30], we consider a time period and truncated stock price domain $\Omega = [0,T] \times [x_{min}, x_{max}]$ into a finite mesh of points $\{t_m | m = 0,\dots,\mathcal{M}\} \times \{x_n | n = 0,\dots,\mathcal{N}-1\}$, where $t_m = m\Delta T$, $\Delta T = {}^T/_{\mathcal{M}}$, $x_n = x_{min} + n\Delta x$, $\Delta x = {}^{(x_{max}-x_{min})}/_{(\mathcal{N}-1)}$. In addition, we keep our simplifying assumption that $x = \log(\frac{S}{S_0})$ or, alternatively, $x = \log(\frac{S}{K})$ when pricing near the strike price is required. Correspondingly, for the frequency grid, we consider a time period and the frequency domain $\hat{\Omega} = [0,T] \times [0, \omega_{max}]$ into a finite mesh of points $\{t_m | m = 0,\dots,\mathcal{M}\} \times \{\omega_n | n = 0,\dots,\mathcal{N}/2\}$, where $\omega_n = n\Delta\omega$, $\Delta\omega = {}^{2\omega_{max}}/_{\mathcal{N}}$, and $\omega_{max} = \frac{1}{2\Delta x}$ according to the Nyquist critical frequency. Since the Fourier transform for negative frequencies is not required[1], the size of the frequency grid is half the size of the spatial grid.

Since discretization on a finite grid involves truncation of the real spatial domain, a localization error is introduced into the numerical algorithm. We truncate the real infinite spatial domain $[0, \infty]$ to the finite domain $[S_{min}, S_{max}]$, where $S_{min} > 0$ and $S_{max} < \infty$. Therefore, asset price values S on the true spatial domain which are outside of the finite domain $[S_{min}, S_{max}]$, i.e. $S < S_{min}$ and $S > S_{max}$, cannot be represented on the truncated discrete spatial domain. Since the real domain of asset prices is not periodic, the solution outside of the domain cannot be replaced by the periodic extension of the solution inside the domain. However, we can obtain an approximate option value at

---

[1] $v(t,x)$ is a real-valued function and, therefore, $\mathcal{F}\left[v^i\right](t,-\omega) = \mathcal{F}\left[v^i\right](t,\omega)$

$S = 0$ by pricing at arbitrarily small values of S_{min} on the expanded grid. Similarly, approximations to the price at $S > S_{max}$ can be obtained by pricing at large values of S_{max} on the expanded grid. Furthermore, since the discrete spatial domain is transformed using the change of variable $x = \log(\frac{S}{S_0})$, the intervals $[S_{min}, \ S_{max}]$ and $[x_{min} \ x_{max}]$ are related so that $S_{min} = S_0 e^{x_{min}}$ and $S_{max} = S_0 e^{x_{max}}$.

4.3.2   Fourier Space Time-stepping Algorithm

Let $v_{m,n}^k \equiv v(t_m, x_n)$ represent the option value $v^k(t,x)$ in regime k at the nodes on the partition of Ω at time t_m in the real log-transformed spatial domain and $F_{m,n}^k \equiv F^k(t_m, \omega_n)$ represent $\mathcal{F}\left[v^k\right](t,\omega)$ at the nodes on the partition of $\hat{\Omega}$ at time t_m in the frequency domain. v_m^k is the vector of option values at time t_m, $\left[v_{m,0}^k, \ldots, v_{m,\mathcal{N}-1}^k\right]$, and F_m^k is the vector of sampled Fourier-transformed option values at time t_m, $\left[F_{m,0}^k, \ldots, F_{m,\mathcal{N}-1}^k\right]^{\mathrm{T}}$. The sampled frequency domain prices can be approximated by applying the discrete Fourier transform (DFT) to the spatial domain as suggested in Surkov [30]:

$$
\begin{aligned}
F_{m,n}^k = \mathcal{F}\left[v^k\right](t_m, \omega_n) &\approx \sum_{j=0}^{\mathcal{N}-1} v_{m,j}^k e^{-i\omega_n x_j} \Delta x \qquad (4.9)\\
&= e^{-i\omega_n x_{min}} \Delta x \sum_{j=0}^{\mathcal{N}-1} v_{m,j}^k e^{-inj/\mathcal{N}}\\
&= \alpha_n \sum_{j=0}^{\mathcal{N}-1} v_{m,j}^k e^{-inj/\mathcal{N}}\\
&= \alpha_n \left[\mathcal{FFT}\left[v_m^k\right]\right]_n,
\end{aligned}
$$

where $\mathcal{F}\left[v^k\right](t_m, \omega_n)$ is a sampled point from the continuous Fourier transform of the option value in the frequency domain, $\alpha_n = e^{-i\omega_n x_{min}}\Delta x$, and $\left[\mathcal{FFT}\left[v_m^k\right]\right]_n$ represents the n-th component of the DFT of the vector v_m^k. The second line of equation (4.9) is obtained by using the Nyquist critical frequency and $x_j = x_{min} + j\Delta x$, $j = 0, \ldots \mathcal{N}-1$.

Having provided the values $F_{m,n}^k$ for all regimes ($k = 1, \ldots, \mathcal{K}$), we have

$$F_{m,n} = \alpha_n \left[\left[\mathcal{FFT} \left[v_m^1 \right] \right]_n, \ldots, \left[\mathcal{FFT} \left[v_m^{\mathcal{K}} \right] \right]_n \right]^{\mathrm{T}} \triangleq \alpha_n \left[\mathcal{FFT} \left[v_m \right] \right]_n, \tag{4.10}$$

where $\left[\mathcal{FFT} \left[v_m \right] \right]_n$ represents the vector of n-th components of the DFTs of the vectors v_m^k (for $k = 1, \ldots, \mathcal{K}$). Furthermore, spatial domain prices are computed from frequency domain prices using a discrete inverse transform denoted by $\mathcal{FFT}^{-1}$:

$$v_{m,n}^k = \left[\mathcal{FFT}^{-1} \left[\alpha^{-1} \cdot F_m^k \right] \right]_n, \text{ where } \alpha = \left[\alpha_0, \alpha_1, \ldots, \alpha_{\mathcal{N}-1} \right]^{\mathrm{T}}. \tag{4.11}$$

Assuming $T = t + \Delta t$, the solution to the transformed PDEs in (4.7) can be re-expressed as

$$F(t, \omega) = e^{\Psi(\omega)\Delta t} F_*, \tag{4.12}$$

where the exponential matrix ($e^{\Psi(\omega)\Delta t}$) is computed for each specific ω separately. Specifically, for any arbitrary values ω_n, t_m as T, and t_{m-1} as t where $t_m = t_{m-1} + \Delta t$, we have

$$F_{m-1,n} = e^{\Psi(\omega_n)\Delta t} F_{m,n} \tag{4.13}$$

where $F_{m-1,n} = F(t_{m-1}, \omega_n)$ is the vector of regime-dependent option values with the k-th element (for regime k) represented by

$$F_{m-1,n}^k = \left(e^{\Psi(\omega_n)\Delta t} F_{m,n} \right)^k, \tag{4.14}$$

The transformation between spatial and frequency domain in equations (4.9) and (4.11) can be combined with solution to the transformed PDEs in (4.12). A one step backward

in time t can be computed by

$$
\begin{aligned}
v_{m-1}^k &= \mathcal{FFT}^{-1}\left[\alpha^{-1} \cdot F_{m-1}^k\right] \qquad\qquad\qquad\qquad\qquad\qquad\qquad\qquad (4.15)\\
&= \mathcal{FFT}^{-1}\left[\alpha^{-1} \cdot \left[F_{m-1,0}^k, \dots, F_{m-1,\mathcal{N}-1}^k\right]^{\mathsf{T}}\right]\\
&= \mathcal{FFT}^{-1}\left[\alpha^{-1} \cdot \left[\left(e^{\Psi(\omega_0)\Delta t}F_{m,0}\right)^k, \dots, \left(e^{\Psi(\omega_{\mathcal{N}-1})\Delta t}F_{m,\mathcal{N}-1}\right)^k\right]^{\mathsf{T}}\right]\\
&= \mathcal{FFT}^{-1}\left[\alpha^{-1} \cdot \left[\alpha_0\left(e^{\Psi(\omega_0)\Delta t}\left[\mathcal{FFT}\left[v_m\right]\right]_0\right)^k, \dots, \alpha_{\mathcal{N}-1}\left(e^{\Psi(\omega_{\mathcal{N}-1})\Delta t}\left[\mathcal{FFT}\left[v_m\right]\right]_{\mathcal{N}-1}\right)^k\right]^{\mathsf{T}}\right]\\
&= \mathcal{FFT}^{-1}\left[\alpha^{-1} \cdot \alpha \cdot \left[\left(e^{\Psi(\omega_0)\Delta t}\left[\mathcal{FFT}\left[v_m\right]\right]_0\right)^k, \dots, \left(e^{\Psi(\omega_{\mathcal{N}-1})\Delta t}\left[\mathcal{FFT}\left[v_m\right]\right]_{\mathcal{N}-1}\right)^k\right]^{\mathsf{T}}\right]\\
&= \mathcal{FFT}^{-1}\left[\left[\left(e^{\Psi(\omega_0)\Delta t}\left[\mathcal{FFT}\left[v_m\right]\right]_0\right)^k, \dots, \left(e^{\Psi(\omega_{\mathcal{N}-1})\Delta t}\left[\mathcal{FFT}\left[v_m\right]\right]_{\mathcal{N}-1}\right)^k\right]^{\mathsf{T}}\right],
\end{aligned}
$$

where, in the third row, $F_{m-1,n}^k$ is replaced by $\left(e^{\Psi(\omega_n)\Delta t} \cdot F_{m,n}\right)^k$ according to (4.14), and then is replaced by its discrete approximation $\left(e^{\Psi(\omega_n)\Delta t}F_{m,n}\right)^k = \alpha_n \cdot \left(e^{\Psi(\omega_n)\Delta t}\left[\mathcal{FFT}\left[v_m\right]\right]_n\right)^k$ according to (4.10), in the fourth row. The coefficient α cancels in the above equation, and can be omitted from the numerical computation.

4.3.3 Wrap-around Error

A truncation error appears when an infinite and continuous asset price domain is represented by a finite and discrete grid. Furthermore, the use of the DFT effectively replaces the original problem by a periodic problem with a period equal to the finite domain size. This may introduce a wrap-around error in the values at the far right end of the domain, $S \gg S_{max}$ and produce spurious option prices at $S \simeq S_{max}$. Similarly, wrap-around pollution in the far left side, $S \ll S_{min}$, leads to spurious option prices at $S \simeq S_{min}$.

4.3.4   Spatial Grid Extension

The spurious option prices near the boundaries can be resolved by extending the real space boundaries. We use the simple expedition of extensions $[x_{min}, x_{max}]$ to $[x^*_{min}, x^*_{max}]$. If $x^*_{max} \gg x_{max}$, a smaller wrap-around pollution, compared to the original non-expanded grid, is expected at x_{max}. Similarly, if $x^*_{min} \ll x_{min}$, the wrap-around effect at x_{min} will be small. However, the downside of the simple extension is that if we use the same number of nodes, the accuracy of the option value generated near the strike price of interest may be reduced.

4.4   American Options

While having the same structure as European options, American options can, however, be exercised at any time prior to expiry. When being exercised, the option gives the holder a payoff depending on the current value of the underlying asset and a fixed strike price. However, it is not rational to exercise when the current payoff is lower than the terminal payoff. American options can be priced either by explicit or penalty methods. The idea of an explicit method, which can be extended to the FST, is to enforce the optimal exercise condition $v^k(\tau, x) \geq v^k(0, x)$, where $k = 1, \ldots, \mathcal{K}$ is the regime number. We apply this condition in the real space and the time step is performed in the Fourier space. Combining the FST algorithm in (4.15) with the optimized early exercise condition yields

$$\nu^k_{m-1} = \mathcal{FFT}^{-1} \left[\left[\left(e^{\Psi(\omega_0)\Delta t} \mathcal{FFT}\,[v_m]_0 \right)^k, \ldots, \left(e^{\Psi(\omega_{\mathcal{N}-1})\Delta t} \mathcal{FFT}\,[v_m]_{\mathcal{N}-1} \right)^k \right]^{\mathrm{T}} \right], \quad (4.16)$$

$$v^k_{m-1} = \max\{\nu^k_{m-1}, v^k_{\mathcal{M}}\}, \quad\quad\quad\quad\quad\quad\quad\quad\quad\quad (4.17)$$

where $\mathcal{FFT}\left[v_m\right]_n = \left[\mathcal{FFT}\left[v_m^1\right]\right]_n, \ldots, \left[\mathcal{FFT}\left[v_m^{\mathcal{K}}\right]\right]_n$ and ν_{m-1}^k denotes the vector of holding values of the option at t_{m-1} before the optimality condition is enforced. The switch between real and Fourier space is inevitable since there is no representation of the max operator in Fourier space.

4.4.1 American Options with Penalty Method

The American option pricing problem is commonly expressed as a linear complementarity problem (LCP) which can be extended to the regime-switching model:

$$
\begin{cases}
(\partial_t + \mathcal{L})v^k(t, x) & \geq 0 \\
v^k - v_*^k & \geq 0 \\
(v^k - v_*^k)(\partial_t v^k + \mathcal{L}\left[v^k\right]) & = 0.
\end{cases} \tag{4.18}
$$

From (4.2), $\mathcal{L}\left[v^k\right]$ is given by

$$
\mathcal{L}\left[v^k\right] = \frac{1}{2}(\sigma^k)^2 v_{xx}^k + (r - \tilde{\eta}^k - \frac{1}{2}(\sigma^k)^2)v_x^k - rv^k + \sum_{l=1, l \neq k}^{\mathcal{K}} \lambda^{kl}\left(v^l(x + \jmath^{kl})\right) - v^k), \tag{4.19}
$$

where v_x^k and v_{xx}^k are the first and second partial derivatives of the option value in regime k, with respect to the log-transformed spatial variable x. The LCP problem (4.18) can be replaced by the penalty method so that

$$
(\partial_t + \mathcal{L})v^k(t, x) + \rho P(v^k)(t, x) = 0, \tag{4.20}
$$

where $P(v^k)(t, x) = \max(v_*^k - v, 0)$ is the penalty function and ρ is a penalty parameter. A Fourier transform can be applied to equation (4.20) in order to resolve the spatial derivative and obtain an ODE:

$$(\partial_t + \Psi(\omega))\mathcal{F}\left[v\right](t,\omega) + \rho\mathcal{F}\left[P(v)\right](t,\omega) = 0, \tag{4.21}$$

where Ψ is the matrix characteristic function as described in (4.5) and

$$\mathcal{F}\left[v\right] = \left[\mathcal{F}\left[v^1\right], \mathcal{F}\left[v^2\right], \ldots, \mathcal{F}\left[v^\mathcal{K}\right]\right]^{\mathrm{T}},$$
$$\mathcal{F}\left[P(v)\right] = \left[\mathcal{F}\left[P(v^1)\right], \mathcal{F}\left[P(v^2)\right], \ldots, \mathcal{F}\left[P(v^\mathcal{K})\right]\right]^{\mathrm{T}}$$

are the regime-dependent vectors in the Fourier space for the option values and penalty functions, respectively. However, due to the nonlinear penalty term in (4.21), an analytical Fourier solution cannot be found. Therefore, we sample the continuous frequency domain prices using a finite number of points in the frequency domain so that

$$(\partial_t + \Psi(\omega_n))\mathcal{F}\left[v\right](t,\omega_n) + \rho\mathcal{F}\left[P(v)\right](t,\omega_n) = 0. \tag{4.22}$$

As in (4.9), the continuous frequency domain prices $(\mathcal{F}\left[v\right](t,\omega_n))$ and penalty value $(\mathcal{F}\left[P(v)\right](t,\omega_n))$ can be approximated by applying the discrete Fourier transform (DFT) to the spatial domain. Assuming $\hat{v} = \left[\hat{v}^1, \ldots, \hat{v}^\mathcal{K}\right]^{\mathrm{T}}$ is the discretized vector of the option values, we obtain $\mathcal{F}\left[v\right](t,\omega_n) = \alpha_n\left[\mathcal{FFT}\left[\hat{v}\right]\right](t,\omega_n)$ and $\mathcal{F}\left[P(v)\right](t,\omega_n) = \alpha_n\left[\mathcal{FFT}\left[P(\hat{v})\right]\right](t,\omega_n)$, where

$$\left[\mathcal{FFT}\left[\hat{v}\right]\right](t,\omega_n) = \left[\left[\mathcal{FFT}\left[\hat{v}^1\right]\right]_n, \ldots, \left[\mathcal{FFT}\left[\hat{v}^\mathcal{K}\right]\right]_n\right]^{\mathrm{T}},$$
$$\left[\mathcal{FFT}\left[P(\hat{v})\right]\right](t,\omega_n) = \left[\left[\mathcal{FFT}\left[P(\hat{v}^1)\right]\right]_n, \ldots, \left[\mathcal{FFT}\left[P(\hat{v}^\mathcal{K})\right]\right]_n\right]^{\mathrm{T}}.$$

This yields

$$(\partial_t + \Psi(\omega_n))\left[\mathcal{FFT}\left[\hat{v}\right]\right](t,\omega_n) + \rho\left[\mathcal{FFT}\left[P(\hat{v})\right]\right](t,\omega_n) = 0. \tag{4.23}$$

Let

$$\hat{F}(t, \omega_n) = [\mathcal{FFT}[(\hat{v})]](t, \omega_n),$$

and

$$\hat{G}(\omega_n) = [\mathcal{FFT}[P(\hat{v})]](\omega_n)$$

be the $\mathcal{K} \times 1$ Fourier-transformed vectors of time-dependent option values and penalty functions, respectively. Then equation (4.23) is replaced by

$$(\partial_t + \Psi(\omega_n))\hat{F}(t, \omega_n) + \rho\hat{G}(\omega_n) = 0, \tag{4.24}$$

where $\hat{G}$ is a function of Forurier-transformed vector of option values $(\hat{G}(\omega_n) = \left[\hat{G}\left[\hat{F}\right]\right](\omega_n))$. Multiplying both sides of the equation by the integrating factor $e^{\Psi(\omega_n)t}$ yields

$$\frac{\partial\left[e^{\Psi(\omega_n)t}\hat{F}(t, \omega_n)\right]}{\partial t} = -\rho e^{\Psi(\omega_n)t}\hat{G}(\omega_n). \tag{4.25}$$

Let $t_m = \Delta t$, $t_{m-1} = 0$, and $\hat{F}_{m,n} = \hat{F}(t_m, \omega_n)$ for the sake of simplicity. Integrating equation (4.25) backwards in time from $t = \Delta t$ to $t = 0$ gives

$$\hat{F}_{m-1,n} - e^{\Psi(\omega_n)\Delta t}\hat{F}_{m,n} = -\rho\int_{t_m=\Delta t}^{t_{m-1}=0} e^{\Psi(\omega_n)t}\hat{G}(\omega_n)dt \tag{4.26}$$

Regarding $\hat{G}(\omega_n)$ as constant, we have

$$\hat{F}_{m-1,n} = e^{\Psi(\omega_n)\Delta t}\hat{F}_{m,n} - \rho\Psi^{-1}(\omega_n)\left[I - e^{\Psi(\omega_n)\Delta t}\right]\hat{G}(\omega_n). \tag{4.27}$$

The non-linear equation in (4.27) cannot be solved easily through analytical methods. Therefore, we solve the equation by a fixed-point iteration scheme. The iterative

equation is given by

$$\left(\hat{F}_{m-1,n}\right)^{(j)} = e^{\Psi(\omega_n)\Delta t}\hat{F}_{m,n} + \rho\Psi^{-1}(\omega_n)\left[e^{\Psi(\omega_n)\Delta t} - I\right]\left(\hat{G}(\omega_n)\right)^{(j-1)} \qquad (4.28)$$

where $e^{\Psi(\omega_n)\Delta t}\hat{F}_{m,n}$ is the current $N \times 1$ regime-dependent vector of option values computed from the previous time step in the Fourier space in which the penalty term is not incorporated. It is interesting to know that we can solve the above equation even if matrix $\Psi(\omega_n)$ is not invertible. After expansion of $e^{\Psi(\omega_n)\Delta t}$,

$$\rho\Psi^{-1}(\omega_n)\left[e^{\Psi(\omega_n)\Delta t} - I\right] \simeq \rho\Psi^{-1}(\omega_n)\left[\left(I + \Psi(\omega_n)\Delta t + \frac{(\Psi(\omega_n))^2(\Delta t)^2}{2!} + \cdots\right) - I\right]$$

$$= \rho(I\Delta t + \frac{\Psi(\omega_n)(\Delta t)^2}{2} + \cdots),$$

so that $\Psi^{-1}(\omega_n)$ does not appear. As in [30], ρ is chosen so that $\rho\Psi^{-1}(\omega_n)\left[e^{\Psi(\omega_n)\Delta t} - I\right] \to I$ as $\Delta t \to 0$. This avoids introducing bias into the explicit iteration. From the first-order Taylor expansion of the exponential function $(e^{\Psi(\omega_n)\Delta t} \simeq I + \Psi(\omega_n)\Delta t)$, we have

$$\rho\Psi^{-1}(\omega_n)\left[e^{\Psi(\omega_n)\Delta t} - I\right] \simeq \rho\Psi^{-1}(\omega_n)\left[\Psi(\omega_n)\Delta t\right]$$

$$= \rho I\Delta t$$

$$\equiv I; \text{ if } \rho\Delta t = 1$$

which results in $\rho = \frac{1}{\Delta t}$. Let

$$\begin{cases} \left(\hat{F}_{m-1,n}\right)^{(0)} &= e^{\Psi(\omega_n)\Delta t}\hat{F}_{m,n}, \\ \left(\hat{F}_{m-1}^k\right)^{(0)} &= \left[\left(\hat{F}_{m-1,0}^k\right)^{(0)}, \ldots, \left(\hat{F}_{m-1,\mathcal{N}-1}^k\right)^{(0)}\right]^{\mathrm{T}}, \end{cases}$$

where k is the regime number, and

$$\begin{cases} \left(\hat{P}_{m-1,n}\right)^{j-1} &= \Psi^{-1}(\omega_n)\left[e^{\Psi(\omega_n)\Delta t} - I\right]\left(\hat{G}_{m-1,n}\right)^{(j-1)}, \\ \left(\hat{P}_{m-1}^k\right)^{j-1} &= \left[\left(\hat{P}_{m-1,0}^k\right)^{j-1}, \ldots, \left(\hat{P}_{m-1,\mathcal{N}-1}^k\right)^{j-1}\right]^{\mathsf{T}}. \end{cases}$$

Equation (4.28) is replaced by

$$\left(\hat{F}_{m-1}^k\right)^{(j)} = \left(\hat{F}_{m-1}^k\right)^{(0)} + \rho\left(\hat{P}_{m-1}^k\right)^{(j-1)}. \tag{4.29}$$

After taking the inverse discrete Fourier transform, the option price in the real space will be

$$\left(\hat{v}_{m-1}^k\right)^{(j)} = \mathcal{FFT}^{-1}\left[\left(\hat{F}_{m-1}^k\right)^{(0)}\right] + \rho\mathcal{FFT}^{-1}\left[\left(\hat{P}_{m-1}^k\right)^{(j-1)}\right].$$

The iterative FST method, therefore, can be expressed as

$$\left(\hat{v}_{m-1}^k\right)^{(j)} = \left(\hat{v}_{m-1}^k\right)^{(0)} + \rho\mathcal{FFT}^{-1}\left[\left(\hat{P}_{m-1}^k\right)^{(j-1)}\right], \tag{4.30}$$

where the initial value $\left(\hat{v}_{m-1}^k\right)^{(0)}$ is computed using the usual time step of the standard FST method given in equation (4.15)

$$\left(\hat{v}_{m-1}^k\right)^{(0)} = \mathcal{FFT}^{-1}\left[\left(\hat{F}_{m-1}^k\right)^{(0)}\right]. \tag{4.31}$$

The iterative scheme of the FST method for the American penalty iteration (4.30) is given in Algorithm 4.1.

Algorithm 4.1 Penalty American Iteration using the FST method (each time step)

```
/* should be assigned out of time-step loop */
```
$\Delta t = \frac{1}{\mathcal{M}}$
$\rho = \frac{1}{\Delta t}$
$TOL = 10^{-6}$

```
/* usual time step of the standard FST method */
For each ω in the frequency domain
```

$$\left(\hat{F}_{m-1}\right)^{(0)} = e^{\boldsymbol{\Psi}\Delta t}\hat{F}_m$$
$$(v_{m-1})^{(0)} = \mathcal{FFT}^{-1}\left[e^{\boldsymbol{\Psi}\Delta t}\hat{F}_m\right]$$

```
End For

/* penalty iteration loop */
For j = 1 until convergence

      For each regime (k)
            /* old option value */
```
$$\left(v_{m-1}^k\right)^{(j-1)} = \mathcal{FFT}^{-1}\left[\left(\hat{F}_{m-1}^k\right)^{(j-1)}\right]$$
```
            /* constructs penalty term from the old option value */
```
$$\left(G_{m-1}^k\right)^{(j-1)} = \mathcal{FFT}\left[max(v_*^k - (v_{m-1}^k)^{(j-1)}, 0)\right]$$
```
      End for

      /* Fourier space: new option value */
      For each ω in the frequency domain
```
$$\left(\hat{F}_{m-1}\right)^{(j)} = \left(\hat{F}_{m-1}\right)^{(0)} + \rho\boldsymbol{\Psi}^{-1}(e^{\boldsymbol{\Psi}\Delta\tau} - I)\left(\hat{G}_{m-1}\right)^{(j-1)}$$
```
      End For

      For each regime (k)
            /* real space: new option value */
```
$$\left(v_{m-1}^k\right)^{(j)} =$$
$$\left(v_{m-1}^k\right)^{(0)} + \rho\mathcal{FFT}^{-1}\left[\left(\boldsymbol{\Psi}^{-1}(e^{\boldsymbol{\Psi}\Delta\tau} - I)\left(\hat{G}_{m-1}\right)^{(j-1)}\right)^k\right]$$
```
      End for
```
$$\text{if } \max_k\left\{\max_n\left(\frac{|v_{m-1,n}^{k,j} - v_{m-1,n}^{k,j-1}|}{max\left(1, |v_{m-1,n}^{k,j-1}|, |v_{m,n}^k|\right)}\right)\right\} < TOL \text{ quit}$$
```
end For /* penalty iteration loop

TERMINAL ITERATE GIVES
```
v_{m-1}^k `FOR` $k = 1, \ldots, \mathcal{K}$

4.5 Expansion of the Matrix Exponential

The matrix exponential ($e^{\Psi \Delta t}$) appearing in the iterative FST method for the European (4.15) and American (4.30) options can be computed in many ways. Moler and Van Loan [26] proposed different methods to compute the exponential of a matrix. We use the `expm` function in Matlab to compute the matrix exponential ($e^{\Psi \Delta t}$). The `expm` function is built-in and implemented using a scaling and squaring algorithm with a Padé approximation as discussed in [26]. Furthermore, we compare our results with the Taylor series expansion of the matrix exponential.

4.5.1 Taylor Series Expansion

The matrix exponential ($e^{\Psi \Delta t}$) can be formally defined by Taylor series

$$e^{\Psi \Delta t} = I + \Psi \Delta t + \frac{\Psi^2 \left(\Delta t\right)^2}{2!} + \cdots, \tag{4.32}$$

where I is the identity matrix. With a small time step ($\Delta t \to 0$), the equation can be approximated by the first two terms so that

$$e^{\Psi \Delta t} \approx I + \Psi \Delta t. \tag{4.33}$$

The same result can be obtained from solving the ODEs in (4.6) by finite difference schemes approximations, such as the forward Euler method

$$\begin{cases} F_{m-1} = (I + \Psi(\cdot)\Delta t)F_m \\ F_{\mathcal{M}} = F_*. \end{cases} \tag{4.34}$$

However, these approximations are only first-order accurate with time-step stability restrictions [30]. We will provide numerical experiments using the first-order Taylor

series in conjunction with the FST method.

4.5.2   Crank-Nicolson Method

The $(1,1)$ Padé approximation[2] to $(e^{\Psi \Delta t})$ [26] gives the second-order Crank-Nicolson scheme

$$e^{\Psi \Delta t} \approx \left(I - \frac{\Psi \Delta t}{2} \right)^{-1} \left(I + \frac{\Psi \Delta t}{2} \right).$$ (4.35)

Taylor expansions gives

$$\left(I - \frac{\Psi \Delta t}{2} \right)^{-1} \left(I + \frac{\Psi \Delta t}{2} \right) \approx I + \Psi \Delta t + \frac{\Psi^2 (\Delta t)^2}{2!} + O\left((\Delta t)^3 \Psi^3 \right),$$ (4.36)

which shows that the Taylor expansion of equation (4.35) agrees with that of the matrix exponential (4.32) through the first three terms. Therefore, the Crank-Nicolson method which corresponds to the $(1,1)$ Padé approximation has second-order global accuracy. Compared to Euler's scheme, this method is both more accurate and unconditionally stable. We will provide numerical experiments using the second-order Crank-Nicolson method in conjunction with the FST method.

4.6   Numerical Experiments

4.6.1   Convergence Results

We price an American put option in a three-state regime-switching model where the underlying jumps in each regime shift. The market is from [23], where the stock follows a Geometric Brownian Motion model within each state. The interest rate and all regime parameters such as volatilities, rate matrix of risk-adjusted intensities, and jump amplitudes are the same as the experiment for the PDE approach in section 3.7.

---

[2]The $(1,1)$ Padé approximation corresponds to the (p, q) Padé approximation where $p = q = 1$.

We consider an American put option with $T = 0.5$ and a strike of $K = 100\$$ which is priced at $S = 100\$$. The results in Tables 4.1, 4.2, and 4.3 suggest that the FST method for pricing American options using an explicit method (equation 4.17) is close to second order in space for each regime. It is, however, possible to obtain an almost-quadratic convergence in time (Table 4.4 and 4.5), if we price American options with the FST method based on the penalty iteration of Forsyth and Vetzal [16]. Furthermore, the matrix exponential function $(e^{\Psi \Delta t})$ in the explicit solution of American options (4.17) has been computed in three ways, the first-order Taylor series approximation method (equation 4.34) in Table 4.1, the second-order Crank-Nicolson method in Table 4.2, and the scaling and squaring algorithm with a Padé approximation method (the `expm` Matlab function) in Table 4.3. It can be seen that the numerical results corroborate the advantage of both the Crank-Nicolson method and the `expm` function in accuracy over the first-order Taylor expansion. The Crank-Nicolson method and the `expm`-based approach provide similar results regarding option values and convergence behaviour. While having a small inconsistency within regimes, the order of convergence is close to 2 in space and time with the penalty formulation as shown in Tables 4.4 and 4.5. There is no significant difference between the computational time costs observed for the Euler, Crank-Nicolson, and `expm`-based approaches. The characteristic matrix (Ψ) is an $\mathcal{K} \times \mathcal{K}$ matrix, with $\mathcal{K} = 3$ in our experiment, and the advantage of the Crank-Nicolson over the `expm` function is not obvious for small amounts of N which is dominated by other time-consuming tasks in the algorithm.

Explicit American - using first-order Taylor series approximation

$\mathcal{N}$	$\mathcal{M}$	Regime 1			Regime 2			Regime 3			
		Value	Change	Ratio	Value	Change	Ratio	Value	Change	Ratio	Time
512	32	3.166310803	0	0	7.96353986	0	0	3.022856693	0	0	0.06
1024	128	3.146209645	0.02010116	0	7.893017717	0.07052214	0	2.997474292	0.02538240	0	0.35
2048	512	3.141177745	0.00503190	3.99	7.875494595	0.01752312	4.02	2.991616938	0.00585735	4.33	2.20
4096	2048	3.139961239	0.00121651	4.14	7.871151027	0.00434357	4.03	2.990281483	0.00133546	4.39	16.00
8192	8192	3.139650762	0.00031048	3.92	7.870070546	0.00108048	4.02	2.989938508	0.00034298	3.89	153.0
16384	32768	3.139570551	0.00008021	3.87	7.869801379	0.00026917	4.01	2.989850548	0.00008796	3.9	1330

Table 4.1: *Explicit-based pricing of a half-year American put option in the three-state market from [23] for consecutive refinements of frequency-time grid. The exponential matrix is computed using a first-order Taylor series expansion. With a small inconsistency within regimes, the order of convergence is very close to 2 in space.*

Explicit American - using Crank-Nicolson approximation

$\mathcal{N}$	$\mathcal{M}$	Regime 1			Regime 2			Regime 3			
		Value	Change	Ratio	Value	Change	Ratio	Value	Change	Ratio	Time
512	32	3.148794578	0	0	7.871543005	0	0	3.0031878	0	0	0.08
1024	128	3.141482182	0.00731240	0	7.870268807	0.00127420	0	2.992330036	0.01085776	0	0.37
2048	512	3.139976982	0.00150520	4.86	7.869848164	0.00042064	3.03	2.99033117	0.00199887	5.43	2.33
4096	2048	3.139654672	0.00032231	4.67	7.869742668	0.00010550	3.99	2.989954899	0.00037627	5.31	19.00
8192	8192	3.139573357	0.00008132	3.96	7.869718709	0.00002396	4.4	2.989856162	0.00009874	3.81	158.0
16384	32768	3.139551059	0.00002230	3.65	7.869713451	0.00005258	4.56	2.989829822	0.00002634	3.75	1480

Table 4.2: *Explicit-based pricing of a half-year American put option in the three-state market from [23] for consecutive refinements of frequency-time grid. The exponential matrix is computed using a second-order Crank-Nicolson method (i.e. (1, 1) Padé approximation). While not consistent within regimes, the order of convergence is close to 2 in space.*

Explicit American - using the `expm` built-in function in Matlab

$\mathcal{N}$	$\mathcal{M}$	*Regime* 1			*Regime* 2			*Regime* 3			
		Value	Change	Ratio	Value	Change	Ratio	Value	Change	Ratio	Time
512	32	3.148502949	0	0	7.870607481	0	0	3.002692149	0	0	0.13
1024	128	3.14145055	0.00705240	0	7.870205119	0.00040236	0	2.992288683	0.01040347	0	0.48
2048	512	3.139971932	0.00147862	4.77	7.869843325	0.00036179	1.11	2.990325832	0.00196285	5.3	2.53
4096	2048	3.139653794	0.00031814	4.65	7.869742303	0.00010102	3.58	2.989953985	0.00037185	5.28	16.80
8192	8192	3.139573029	0.00008077	3.94	7.869718658	0.00002365	4.27	2.989855813	0.00009817	3.79	173.0
16384	32768	3.139550971	0.00002206	3.66	7.869713441	0.00000522	4.53	2.989829728	0.00002609	3.76	1400

Table 4.3: *Explicit-based pricing of a half-year American put option in the three-state market from [23] for consecutive refinements of frequency-time grid. The exponential matrix is computed using the* `expm` *built-in function in Matlab, at each point of space for every time step. While not consistent within regimes, the order of convergence is close to 2 in space.*

Penalty American - using Crank-Nicolson approximation

$\mathcal{N}$	$\mathcal{M}$	*Regime* 1			*Regime* 2			*Regime* 3			
		Value	Change	Ratio	Value	Change	Ratio	Value	Change	Ratio	Time
512	32	3.151069537	0	0	7.873519757	0	0	3.004542206	0	0	0.222
1024	64	3.142099459	0.00897008	0	7.870774691	0.00274507	0	2.992838725	0.0117035	0	0.783
2048	128	3.140178324	0.00192113	4.67	7.869972197	0.00080249	3.42	2.990488293	0.00235043	4.98	3.05
4096	256	3.139732602	0.00044572	4.31	7.869774865	0.00019733	4.07	2.990015103	0.00047319	4.97	13.5
8192	512	3.139605794	0.00012681	3.51	7.869726514	4.84E-05	4.08	2.989881142	0.00013396	3.53	56.9
16384	1024	3.139565957	3.98E-05	3.18	7.869715152	1.14E-05	4.26	2.989841402	3.97E-05	3.37	285

Table 4.4: *Penalty-based pricing of a half-year American put option in the three-state market from [23] for consecutive refinements of frequency-time grid. The exponential matrix is computed using the Crank-Nicolson method, at each point of space for every time step. While not consistent within regimes, the order of convergence is close to 2 in space and 2 in time. The time-step, penalty parameter, and convergence tolerance values are* $\Delta T = \frac{T}{\mathcal{M}}$, $\rho = \frac{1}{\Delta T}$, *and* $TOL = 10^{-6}$, *respectively. The penalty parameter* $(\rho = \frac{1}{\Delta T})$ *gives a smooth rate of convergence. The penalty loop converges in 1-3 iterations.*

Penalty American - using the `expm` built-in function in Matlab

$\mathcal{N}$	$\mathcal{M}$	Regime 1			Regime 2			Regime 3			
		Value	Change	Ratio	Value	Change	Ratio	Value	Change	Ratio	Time
512	32	3.150926911	0	0	7.872529927	0	0	3.004346253	0	0	0.28
1024	64	3.142034767	0.00889214	0	7.870523601	0.00200633	0	2.992762317	0.0115839	0	0.925
2048	128	3.140169995	0.00186477	4.77	7.869907678	0.00061592	3.26	2.990478353	0.00228396	5.07	3.49
4096	256	3.139731212	0.00043878	4.25	7.869758151	0.00014953	4.12	2.990013128	0.00046523	4.91	13.5
8192	512	3.139605673	0.00012554	3.50	7.869722127	3.60E-05	4.15	2.989880768	0.00013236	3.51	64
16384	1024	3.139566084	3.96E-05	3.17	7.869713917	8.21E-06	4.39	2.989841426	3.93E-05	3.36	281

Table 4.5: *Penalty-based pricing of a half-year American put option in the three-state market from [23] for consecutive refinements of frequency-time grid. The exponential matrix is computed using the* `expm` *built-in function in Matlab, at each point of space for every time step. While not consistent within regimes, the order of convergence is close to 2 in space and 2 in time. The time-step, penalty parameter, and convergence tolerance values are* $\Delta T = \frac{T}{\mathcal{M}}$, $\rho = \frac{1}{\Delta T}$, *and* $TOL = 10^{-6}$, *respectively. The penalty parameter (*$\rho = \frac{1}{\Delta T}$*) gives a smooth rate of convergence. The penalty loop converges in 1-3 iterations.*

4.6.2 Wrap-around Error Observations

The pricing of American put options under the three-regime model in the previous section is investigated when the asset is near the boundaries. We expect an almost-zero value for the price of American put options at large values of asset price S. However, running the FST algorithm with the real space boundaries $x_{min} = -7.5$ and $x_{max} = 7.5$ produces significant wrap-around error at the right boundary of the domain near $S = S_{max} = 1.808 * 10^5$. The spurious option prices at the extreme right side of the domain when S is approximately greater than $1.6 * 10^5$ ($S \gtrapprox 1.6 * 10^5$) can be observed in Table 4.6. On the contrary, there is no considerable difference between the price of American put options at small values of asset price S in the original grid ($S = 0.0553$ in Table 4.6) and the correspondent price coming from the expanded grid ($S = 0.05$ in Table 4.7). Therefore, no wrap-around error was observed at the left boundary of the domain near $S = S_{min} = 0.0553$. The absence of the wrap-around error at the left side of the domain might be due to the application of the American constraint. However, although early

exercise is allowed everywhere, the algorithm is not effected by the American constraint for large values of S near S_{max} since the payoff $(\max(K - S, 0))$ is likely to be zero.

Wrap-around effects near the boundaries when $\{x_{min}, x_{max}\} = \{-7.5,\ 7.5\}$ has been resolved by expanding the real space boundaries. The new expanded boundaries $(\{-15,\ 15\})$ allowed us to evaluate option prices over a greater domain. As shown in Table 4.7, running the FST algorithm with the new expanded boundaries resolves the wrap-around error near the original boundaries $(S = 0.05,\ S = 2 * 10^5)$. However, the accuracy of the option value generated near the strike price of interest has been reduced. For instance, when $S = 100$ and $(\mathcal{N}, \mathcal{M}) = (512, 32)$ points in the space-time grid, the option price with the original boundaries $(V = 3.150743)$ is closer to its converged value $(V = 3.139596)$. Evaluated with the expanded boundaries, however, the option price $(V = 3.207299)$ and its converged value $(V = 3.139697)$ are more distant. An insightful comparison between the rows of Tables 4.6 and 4.7 shows that the reduction in accuracy has been treated by choosing a condensed grid. It can be observed that the option values in the first row (i-th row) of Table 4.6 are correspondent, in terms of accuracy, to the values in the second row $((i + 1)$-th row) of Table 4.7.

The wrap-around effects, however, can be still observed in the divergent option prices near the new extended right boundaries $(S \gtrapprox 3 * 10^8)$. Similarly, no wrap-around error was observed at the left boundary of the domain near $S = S_{min} = 3.059 * 10^{-5}$.

Wrap-around Effects ($x = [-7.5, 7.5]$)

$\mathcal{N}$	$\mathcal{M}$	$S_{min} =$ 0.0553	$S = 0.1$	$S = 100$	$S = 10^5$	$S =$ $1.6 * 10^5$	$S =$ $1.7 * 10^5$	$S_{max} =$ $1.808 * 10^5$
		Value	Value	Value	Value	Value	Value	Value
512	32	99.538479	99.897984	3.150743	0.189475	4.34	28.52	76.76
1024	64	99.337753	99.899795	3.141975	0.073808	5.30	35.70	86.87
2048	128	99.258271	99.900068	3.140141	0.024847	6.08	39.62	92.88
4096	256	99.603551	99.899998	3.139712	0.007857	6.63	41.72	96.08
8192	512	99.529701	99.900001	3.139596	0.002383	6.97	42.85	97.71
16384	1024	99.549449	99.900000	3.139562	0.000646	7.17	43.45	98.62

Table 4.6: *Wrap-around effects on the penalty-based pricing of a half-year American put option with the usual real space boundaries $\{x_{min}, x_{max}\} = \{-7.5, 7.5\}$, in the first regime of the three-state market from [23], for consecutive refinements of frequency-time grid. The wrap-around effects can be observed in the divergent option prices near the right boundaries ($S \gtrapprox 1.6 * 10^5$).*

Resolving Wrap-around Effects after Extension ($x = [-15, 15]$)

$\mathcal{N}$	$\mathcal{M}$	$S_{min} =$ $3.059 * 10^{-5}$	$S =$ $4 * 10^{-5}$	$S = 0.05$	$S = 100$	$S =$ $2 * 10^5$	$S = 2 * 10^8$	$S =$ $3 * 10^8$	$S_{max} =$ $3.269 * 10^8$
		Value	Value	Value	Value	Value	Value	Value	Value
512	32	99.916945	100.610538	**99.949964**	3.207299	**0.017621**	0.406915	9.05	57.27
1024	64	99.888505	100.323618	**99.949969**	3.150712	**0.012866**	0.239252	14.52	76.97
2048	128	99.821430	100.007707	**99.950022**	3.141984	**0.004972**	0.092323	19.43	87.21
4096	256	99.713993	100.000028	**99.949995**	3.140111	**0.001593**	0.033326	22.33	93.09
8192	512	99.887777	100.000002	**99.950000**	3.139697	**0.000489**	0.012792	23.96	96.40
16384	1024	99.82917064	99.99996078	**99.94469999**	3.139588	**0.000140**	0.006138	24.85	98.03

Table 4.7: *Wrap-around effects on the penalty-based pricing of a half-year American put option with the extended real space boundaries $\{x_{min}, x_{max}\} = \{-15, 15\}$, in the first regime of the three-state market from [23], for consecutive refinements of frequency-time extended grid. There is no wrap-around error near the old boundaries ($S = 0.05, S = 2 * 10^5$) after extension. The wrap-around effects, however, can be still observed in the divergent option prices near the new extended right boundaries ($S \gtrapprox 3 * 10^8$).*

Chapter 5

Comparisons

We compare the analytical, PDE, and FST approaches developed for pricing options in a regime-switching market. Since there is no analytical solution for pricing American options in a regime market, the comparison is undertaken with the PDE solution of European options.

Model Specifications			
Option type	*European call*	regime volatilities	$\sigma = \{0.25, 0.15\}$
T	*1 year*	intensities	$\lambda^{h \to l} = \lambda^{l \to h} = 0.5$
Model	*2-state*	PDE Method	*fixed point*
interest rate	$r = 0.05$	PDE timestep	*variable*

Table 5.1: *Input model specifications and parameters for comparison of Analytical and PDE approaches.*

Parameters are given in Table 5.1. Table 5.2 compares the analytical and PDE solutions for pricing a 1-year European call option, priced at $S = 100\$$ with a strike of $K = 100\$$, under a two-state regime-switching model. A significant improvement, as we expect, can be observed for the analytical approach in terms of the rate of convergence and computations.

Comparison of Analytical and PDE approaches

		Analytical Approach							PDE Approach				
		(Regime 1)		(Regime 2)		Time			(Regime 1)		(Regime 2)		Time
n_1	n_2	Option Value	Ratio	Option Value	Ratio	(s)	$\mathcal{N}$	$\mathcal{M}$	Option Value	Ratio	Option Value	Ratio	(s)
8	2	8.402481339		6.459199965		0.03	100	138	11.69943264		9.336093165		0.1
8	4	12.47095306		10.04096878		0.6	200	277	11.70364712		9.338455707		0.3
8	8	11.65982478	5.02	9.314436934	4.93	0.11	400	555	11.70471460	3.95	9.339051175	3.97	1.0
8	16	11.70631441	17.45	9.340478131	27.9	0.19	800	1110	11.70498246	3.99	9.339200391	3.99	4.0
8	32	11.70507316	37.45	9.339251689	21.2	0.31	1600	2218	11.70504949	4.00	9.339237717	4.00	16.1
8	64	11.70507184	940.3	9.339250161	803	0.58	3200	4434	11.70506625	4.00	9.339247050	4.00	63.5
8	128	11.70507184	NA	9.339250161	NA	1.25	6400	8866	11.70507044	4.00	9.339249383	4.00	241.1

Table 5.2: *Comparison of the analytical and PDE approaches in a 2-state regime-switching model for pricing European call options. Data is given in Table 5.1. The analytical and PDE solutions are given in Proposition 1 (Chapter 2) and Algorithm 3.1, respectively. n_1 and n_2 are used for the Gaussian approximation of the analytical solution. $\mathcal{N}$ and $\mathcal{M}$ are the size of grid and number of timesteps in the numerical PDEs.*

5.1 American Pricing Problem

Parameters are given in Table 5.3. Table 5.4 gives the comparison of the FST and PDE solutions for pricing a half-year American put option under a three-state regime-switching model. Since we have developed several methods in each case, only the most efficient methods among both the FST and PDE approaches are chosen for the sake of comparison. As given in Table 5.3, the Crank-Nicolson method with the penalty formulation and the fixed point-policy with the penalty formulation and a variable timestepping are the efficient FST and PDE choices, respectively.

Model Specifications			PDE values	FST values
Option type	*American put*	Method	*fixed point*	*Crank-Nicolson*
T	*0.5 year*	Formulation	*penalty*	*penalty*
Parameters	*3-state from [23]*	Timestep	*variable*	$\Delta T = \frac{T}{\mathcal{M}}$
		Penalty parameter	$\varepsilon = 10^{-6}\Delta\tau$	$\rho = \frac{1}{\Delta T}$
		Tolerance	$tol = 10^{-8}$	$tol = 10^{-6}$

Table 5.3: *Input model specifications and parameters for comparison of FST and PDE approaches.*

PDE approach

		Jump							No Jump				
$\mathcal{N}$	$\mathcal{M}$	Value	Ratio			Time	$\mathcal{N}$	$\mathcal{M}$	Value	Ratio			Time
		(Reg. 2)*	(1)**	(2)	(3)	(s)			(Reg. 2)	(1)	(2)	(3)	(s)
100	146	7.876208010				0.2	100	43	1.531024768				0.1
200	294	7.871012198				0.6	200	81	1.533292053				0.2
400	589	7.870074165	41.88	5.54	37.39	2.2	400	157	1.533870737	3.87	3.92	3.88	0.6
800	1178	7.869812031	576	3.58	49.63	7.7	800	307	1.534017315	3.91	3.95	3.91	2.4
1600	2356	7.869726457	9.12	3.06	4.00	31.3	1600	607	1.534054238	3.97	3.97	3.95	9.0
3200	4712	7.869715397	3.97	7.74	3.86	126.2	3200	1206	1.534063562	3.97	3.96	3.96	33.1

* Reg. = Regime

** 1 = Regime 1

Table 5.4: *Comparison of the PDE approach in a 3-state regime-switching market (with jumps and no jumps) for pricing American options. Input data is referred or given in Table 5.3.*

FST approach

		Jump							No Jump				
$\mathcal{N}$	$\mathcal{M}$	Value	Ratio			Time	$\mathcal{N}$	$\mathcal{M}$	Value	Ratio			Time
		(Reg. 2)	(1)	(2)	(3)	(s)			(Reg. 2)	(1)**	(2)	(3)	(s)
512	128	7.872785648				0.459	512	128	1.557821340				0.485
1024	256	7.870604623				1.63	1024	256	1.539593671				1.65
2048	512	7.869921796	4.47	3.19	4.71	6.39	2048	512	1.535333697	5.79	4.28	5.58	6.14
4096	1024	7.869760631	4.47	4.24	5.05	25.5	4096	1024	1.534392840	4.02	4.53	4.33	24.4
8192	2048	7.869723039	4.17	4.29	4.14	114	8192	2048	1.534148985	4.00	3.86	4.11	124
16384	4096	7.869714247	3.70	4.28	3.81	655	16384	4096	1.534087606	4.19	3.97	4.27	649

Table 5.5: *Comparison of the FST approach in a 3-state regime-switching market (with jumps and no jumps) for pricing American options. Input data is referred or given in Table 5.3.*

Although suffering from a small inconsistency within regimes, the ratio of convergence is close to second order for each consecutive refinement in the FST approach. However, the quadratic-expected rate of convergence is not consistent within regimes and sometimes oscillatory for each consecutive refinement in the PDE approach. The right parts of Tables 5.4 and 5.5 represent these two approaches with a no-jump assumption in the asset price. It can be seen that the FST method is more stable than the PDE method upon changes in the model parameters. While the assumption of no jump

has no significant impact on the former in terms of the rate of convergence, the latter benefits from a significant improvement regarding the convergence consistency within regimes. A quadratic rate of convergence in each refinement with a consistency within all regimes can be observed with the no-jump case in the PDE solution of Table 5.4. The decrease in the amount of work for the PDE approach is explained by the difference in the number of timesteps for the jump and no-jump cases. Specifically, a grid of size 3200 with 1206 timesteps requires 33.1 seconds to compute the no-jump option values while the same grid with 4712 timesteps (3.9 times the no-jump timesteps) takes 126.2 seconds (3.8 times the no-jump cost) for the PDE solution when jumps are allowed.

Chapter 6

Conclusions

We have computed the analytical solution for pricing European options under a two-state regime-switching model. As expected, the rate of convergence is exponential and the feature of implied volatility, volatility smile, can be captured through this model. No analytical solution has been found for pricing American options or even European options with more than two states in the model. Therefore, numerical techniques are used as alternative pricing tools for both American and k-state ($k > 2$) European options.

In this thesis, several PDE and FST algorithms have been developed. A brief comparison between numerical PDE solutions demonstrates that:

- The full policy combined with a simple iteration, and fixed point-policy iteration methods have better performance than other techniques in terms of computational costs.

- A direct solution for solving the linear system appearing in the full policy iteration is the most expensive approach.

- Oscillatory convergence rates for the consecutive refinements within regimes are observed for all PDE solutions.

- The assumption of no jump in the model eliminates both the oscillation and inconsistency in the convergence rates.

- Having been compared with the no-jump case, sparsity patterns show that the amount of fill-in in the LU factorization is significantly less than that of the model with jumps. This explains the reduction in operation count for the no-jump model.

Having been formulated using the penalty method, the fixed point-policy iteration and the FST method in conjunction with the Crank-Nicolson approximation are chosen for the sake of comparison. In particular:

- In terms of the convergence behaviour, although not consistently second order in the ratio of convergence, the FST method performs better than the PDE method even if jumps are allowed to occur.

- The FST method is more stable than the PDE method upon changes in the model parameters. The assumption of no-jump leads to a consistent and non-oscillatory convergence rates in the PDE approach.

- While option values are always accurate in the PDE approach, the wrap-around effect in the FST method leads to inaccurate results near the boundaries.

6.1   Future Work

Some directions in which further research are as follow:

- The wrap-around effect caused by the periodic extension of the FST solution inside the domain is solved by a domain extension. The domain extension involves with more computations which is not necessarily the most efficient work around.

- Model parameters are extracted from a calibration process. Calibrating a regime-switching model is a challenging work.

References

[1] Giovanni Barone-Adesi and Robert E. Whaley. Efficient analytic approximation of American option values. *The Review of Finance*, XLII(2):301–320, 1987. 3

[2] W. Barrett. Convergence properties of gaussian quadrature formulae. *The Computer Journal*, 3(4):227–277, 1961. 13

[3] F. Black and M. Scholes. The pricing of options and corporate liabilities. *Journal of Political Economy*, 81:639–659, 1973. 1

[4] Olivier Bokanowski, Stefania Maroso, and Hasnaa Zidani. Some convergence results for Howard's algorithm. *SIAM Journal of Numerical Analysis*, 47(4):3001–3026, 2009. 29, 38

[5] Nicolad P.B. Bollen. Valuing options in regime-switching models. *Journal of Derivatives*, 6:38–49, Fall 1998. 2

[6] Phelim Boyle and Thangaraj Draviam. Pricing exotic options under regime switching. *Insurance: Mathematics and Economics*, 40:267–282, 2007. 3, 9

[7] John Buffington and Robert J. Elliott. American options with regime switching. *International Journal of Theoretical and Applied Finance*, 5:497–514, 2002. 3

[8] Peter Carr. Randomization and the American put. *The Review of Financial Studies*, 11:597–626, 1998. 5

[9] Shan Chen and Margaret Insley. Regime switching in stochastic models of commodity prices: an application to an optimal tree harvesting problem. 2008. 3

[10] Zhuliang Chen and Peter A. Forsyth. Implications of a regime-switching model on natural gas storage valuation and optimal operation. *Journal of Quantitative Finance*, 10(2):159–176, 2010. 3

[11] Timothy A. Davis. *Direct Methods for Sparse Linear Systems*. SIAM, Philadelphia, Pennsylvania, 2006. 35

[12] Y. d'Halluin, P. A. Forsyth, and K. R. Vetzal. Robust numerical methods for contingent claims under jump diffusion processes. *IMA Journal on Numerical Analysis*, 25:87–112, 2005. 26

[13] Jin-Chuan Duan, Ivilina Popova, and Peter Ritchken. Option pricing under regime switching. *Quantitative Finance*, 2:116–132, 2002. 3

[14] Robert J. Elliott, Tak Kuen Siu, and Leunglung Chan. A PDE approach for risk measures for derivatives with regime switching. *Annals of Finance*, 4:55–74, 2008.

[15] P. A. Forsyth. *SparseIt++ user guide*. Department of Computer Science, University of Waterloo, august 20 edition, 2002. 36

[16] P. A. Forsyth and K. Vetzal. Quadratic convergence of a penalty method for valuing American options. *SIAM Journal of Scientific Computing*, 23:2095–2122, 2002. 28, 68

[17] J. Hamilton. Analysis of time series subject to changes in regime. *Journal of Econometrics*, 45:39–79, 1990. 2

[18] Mary R. Hardy. A regime-switching model of long-term stock returns. *North American Actuarial Journal*, 5:41–53, 2001. 2, 3

[19] Y. Huang, P.A. Forsyth, and G. Labahn. Combined fixed point and policy iteration for hjb equations in finance. 2010. 36

[20] Y. Huang, P.A. Forsyth, and G. Labahn. Methods for pricing american options under regime switching. 2011. 29, 34, 36, 37

[21] Bong-Gyu Jang. American put options with regime-switching volatility. Working paper, Social Science Research Network, 2005.

[22] Bong-Gyu Jang and Kum-Hwan Roh. Valuing qualitative options with stochastic volatility. *Quantitve Finance*, 9(7):819–825, 2009. 3, 5

[23] J. Shannon Kennedy. *Hedging Contingent Claims in Markets with Jumps*. PhD thesis, David R. Cheriton School of Computer Science, University of Waterloo, 2007. 1, 2, 7, 19, 21, 22, 23, 26, 37, 40, 41, 42, 43, 44, 45, 46, 47, 48, 49, 52, 67, 69, 70, 71, 73, 75

[24] A. Q. M. Khaliq and R.H. LIU. New numerical scheme for pricing American option with regime-switching. *International Journal of Theoretical and Applied Finance*, 12(3):319–340, 2009. 3, 21

[25] H. Le and C. Wang. Quadratic convergence of a penalty method for valuing American options. *SIAM Journal of Scientific Computing*, 23:2095–2122, 2002. 3

[26] Cleve Moler and Charles Van Loan. Nineteen dubious ways to compute the exponential of a matrix, twenty-five years later. *SIAM Review*, 45(1):3–49, 2003. 66, 67

[27] Vasanttilak Naik. Option valuation and hedging strategies with jumps in the volatility of asset returns. *The Journal of Finance*, XLVIII(5):1969–1984, 1993. 2, 3, 4, 5, 6, 7, 8, 17

[28] Y. Saad. Iterative methods for sparse linear systems. *SIAM*, 2003. 36

[29] E. S. Schwartz. The stochastic behaviour of commodity prices. *The Journal of Finance*, 52(3):923–973, 1997. 3

[30] Vladimir Surkov. *Option Pricing Using Fourier Space Time-Stepping Framework*. PhD thesis, Department of Computer Science, University of Toronto, 2009. 3, 52, 55, 56, 63, 66

[31] Z. Xu. Stochastic models for gas prices. Master's thesis, Department of Mathematics and Statistics, University of Calgary, 2004. 3

[32] Fahuai Yi. American put option with regim-switching volatility (finite time horizon)—variational inequality approach. *Mathematical Methods in the Applied Sciences*, 31:1461–1477, 2008.

[33] Fei Lung Yuen and Hailiang Yang. Option pricing with regime switching by trinomial tree method. *Journal of Computational and Applied Mathematics*, 233(8):1821–1833, 2010.

[34] R. Zvan, P. A. Forsyth, and K. R. Vetzal. Penalty methods for American options with stochastic volatility. *Journal of Computational and Applied Mathematics*, 91:199–218, 1998. 21